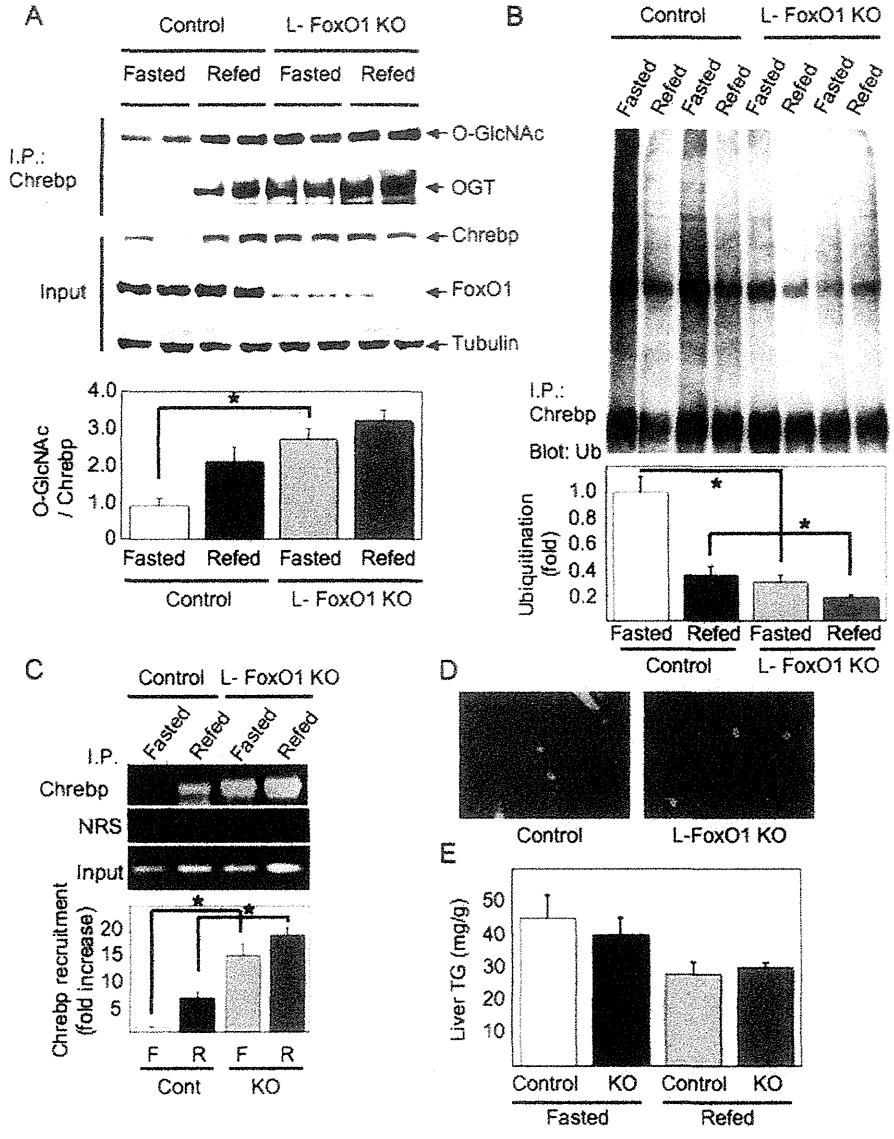

Figure 3. Chrebp O-glycosylation, protein stability, and recruitment to the L-PK promoter are increased in FoxO1 knockout liver. (A and B) The liver samples isolated from L-FoxO1-KO and the control mice at the points of 24 hr fasted or 3 hr refed after 24 hr starvation were subjected to immunoprecipitation with anti-Chrebp antibody followed by blotting with anti-O-GlcNAc, anti-OGT (A) or anti-ubiquitin antibody (B). Input indicates the expression levels of Chrebp, FoxO1 or tubulin. Quantitative analyses were performed by assessment of O-glycosylation (A) or ubiquitination (B) levels compared with the protein level of Chrebp using densitometry, showing as a bar graph below the results of blotting. (C) The liver extracts were also subjected to chromatin immunoprecipitation assay using anti-Chrebp antibody and primers for the L-PK promoter. Quantitative analyses were performed using densitometry. Input indicates extracted DNA prior to immunoprecipitation. Experiments were repeated at least three times. Data represent mean ± SEM. *P<0.05. (D) Hematoxylin-and-eosin (H-E) staining of the liver sections from 24 hr fasted L-FoxO1-KO and the control mice. Magnification, x100. (E) Hepatic triglyceride (TG) contents in 24 hr fasted or 3 hr refed (after 24 hr starvation) L-FoxO1-KO and the control mice (n = 6 for each group). Data represent mean ± SEM.
doi:10.1371/journal.pone.0047231.g003

promoter was enhanced in the liver of L-FoxO1-KO mice compared with controls (Fig. 3C), consistent with our previous results showing that *Lpk* mRNA was increased in liver-specific FoxO1 knockout mice [11].

We next investigated the physiological consequences of FoxO1 ablation in the liver. Because we showed FoxO1 ablation in the liver enhanced Chrebp protein stability and Chrebp recruitment to its target gene promoter, we predicted that hepatic lipid contents should be increased in L-FoxO1-KO mice. However, histological analysis using the liver sections showed no morphological difference between L-FoxO1-KO and control mice (Figure 3D). Furthermore, hepatic triglyceride contents were unchanged in L-FoxO1-KO mice in both fasted and refed conditions (Figure 3E).

Discussion

Our studies identify a direct molecular link between insulin signaling pathways regulating hepatic glucose production and those regulating glycolysis and lipogenesis. In addition to Chrebp, another critical transcription factor for lipogenesis is sterol regulatory element-binding protein 1c (Srebp-1c) [20]. Although the transcriptional activity of Srebp-1c is mainly regulated by the cleavage of its NH_2-terminal domain and nuclear translocation [21], it is also known that Srebp-1c is regulated by insulin at the transcriptional level via liver X receptor (LXR) [22]. Recently, it has been shown that Chrebp, like Srebp-1c, is a direct target of LXR [23], indicating that Chrebp may be also regulated at the transcriptional level by insulin. Our data demonstrate a different mechanism of regulation, as we show that protein, but not mRNA levels of Chrebp are regulated by various metabolic conditions in primary hepatocytes and mouse liver. We also show that Chrebp is O-glycosylated by high glucose (in hepatocytes) and re-feeding (in liver), leading to increased protein level of Chrebp, owing to decreased ubiquitination.

Glucose taken into hepatocytes is mainly converted to pyruvate or glycogen to produce or store energy. However, excess glucose enters into hexosamine biosynthetic pathway (HBP), leading to the production of UDP-N-acetylglucosamine (UDP-GlcNAc). By using UDP-GlcNAc as the donor substrate, O-GlcNAc transferase (OGT) catalyzes O-glycosylation modification of proteins on Ser/Thr residues. Although only ~2–3% of intracellular glucose enters the HBP [24], it is known that hyperglycemia increases glucose flux into HBP and subsequent O-glycosylation of various proteins [25]. Furthermore, transgenic mice overexpressing OGT show diabetic phenotype due to insulin resistance [26]. Taken together, these data suggest that the increase in O-glycosylation is associated with the pathophysiology of diabetes. Recently, three key transcription factors for glucose metabolism, FoxO1, Pgc-1α and Torc2 (Crtc2) have been reported to be regulated by O-glycosylation modification [27–30]. Furthermore, Guinez et al. reported that Chrebp is also regulated by O-glycosylation, leading to the increase in Chrebp protein level and its transcriptional activity [19].

FoxO1 is a member of the forkhead box containing protein of the O subfamily, which regulates metabolism as well as cellular proliferation, apoptosis, differentiation and stress resistance [4]. FoxO1 transcriptional activity is regulated by insulin through phosphorylation by Akt and following nuclear exclusion [31–33]. We previously reported that FoxO1 plays a central role in regulating glucose production in liver through the regulation of gluconeogenic genes, such as glucose-6-phosphatase (G6Pase) and phosphoenolpyruvate-carboxykinase (PEPCK) [34] [12]. We also previously reported that hepatic FoxO1 ablation leads to slight increases in *Fasn* and *Lpk*, two critical Chrebp targets, without affecting *Chrebp* mRNA levels [11]. Thus, in addition to the function of FoxO1 to increase gluconeogenesis, we propose here that FoxO1 also decreases glucose utilization and lipid synthesis by reducing Chrebp activity. Because insulin essentially inhibits FoxO1 transcriptional activity through nuclear exclusion, insulin increases glucose utilization and lipid synthesis as well as decreases glucose production (Fig. 4).

In this study, we showed FoxO1 ablation in the liver enhanced Chrebp protein stability and Chrebp recruitment to its target gene promoter. Therefore we predicted that hepatic lipid synthesis should be increased in L-FoxO1-KO mice. However, hepatic lipid contents were unchanged in these mice (Fig. 3D and 3E). One possible explanation for this phenotype was that because hyperglycemia-induced oxidative stress leads to FoxO1 activation by acetylation-dependent mechanism as we previously reported [13], the effect of FoxO1 on lipid metabolism might only become apparent in hyperglycemic conditions. Another explanation was that because not only Chrebp but also Srebp1c or LXR contribute to the regulation of hepatic lipid metabolism, the effect of FoxO1 ablation might be compensated by the other factors *in vivo*.

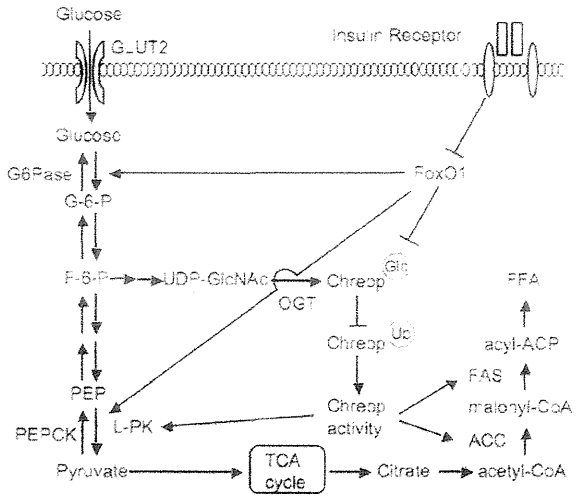

Figure 4. Proposed model for the role of FoxO1 integrating glucose utilization and lipid synthesis through regulation of Chrebp O-glycosylation.
doi:10.1371/journal.pone.0047231.g004

Considering that different amino acid residues are targeted by O-glycosylation (Ser/Thr) *vs.* ubiquitination (Lys), it remains unclear how increased O-glycosylation is associated with decreased ubiquitination of Chrebp. However, one possible mechanism is that O-glycosylation may change protein structure, affecting the susceptibility of ubiquitination and subsequent protein degradation [35]. In future studies, it will be of importance to unveil the mechanism by which FoxO1 inhibits Chrebp O-glycosylation.

Acknowledgments

We thank C. Osawa for excellent technical assistance and members of the Accili and Kitamura laboratories for stimulating discussions. Correspondence and requests for materials should be addressed to T.K.

Author Contributions

Conceived and designed the experiments: YI-K TK. Performed the experiments: YI-K TS MK H-JK Y-SL OK HY-H KI. Analyzed the data: YI-K TS MK DA TK. Contributed reagents/materials/analysis tools: YI-K TS MK HY-H KI. Wrote the paper: DA TK.

References

1. Lin HV, Accili D (2011) Hormonal regulation of hepatic glucose production in health and disease. Cell Metab 14: 9–19.
2. Ferre P, Foufelle F (2010) Hepatic steatosis: a role for de novo lipogenesis and the transcription factor SREBP-1c. Diabetes Obes Metab 12 Suppl 2: 83–92.
3. Haeusler RA, Accili D (2008) The double life of Irs. Cell Metab 8: 7–9.
4. Accili D, Arden KC (2004) FoxOs at the Crossroads of Cellular Metabolism, Differentiation, and Transformation. Cell 117: 421–426.

5. Shin DJ, Osborne TF (2009) FGF15/FGFR4 integrates growth factor signaling with hepatic bile acid metabolism and insulin action. J Biol Chem 284: 11110–11120.
6. Uyeda K, Repa JJ (2006) Carbohydrate response element binding protein, ChREBP, a transcription factor coupling hepatic glucose utilization and lipid synthesis. Cell Metab 4: 107–110.
7. Yamashita H, Takenoshita M, Sakurai M, Bruick RK, Henzel WJ, et al. (2001) A glucose-responsive transcription factor that regulates carbohydrate metabolism in the liver. Proc Natl Acad Sci U S A 98: 9116–9121.
8. Ishii S, Iizuka K, Miller BC, Uyeda K (2004) Carbohydrate response element binding protein directly promotes lipogenic enzyme gene transcription. Proc Natl Acad Sci U S A 101: 15597–15602.
9. Kabashima T, Kawaguchi T, Wadzinski BE, Uyeda K (2003) Xylulose 5-phosphate mediates glucose-induced lipogenesis by xylulose 5-phosphate-activated protein phosphatase in rat liver. Proc Natl Acad Sci U S A 100: 5107–5112.
10. Kawaguchi T, Takenoshita M, Kabashima T, Uyeda K (2001) Glucose and cAMP regulate the L-type pyruvate kinase gene by phosphorylation/dephosphorylation of the carbohydrate response element binding protein. Proc Natl Acad Sci U S A 98: 13710–13715.
11. Haeusler RA, Han S, Accili D (2010) Hepatic FoxO1 ablation exacerbates lipid abnormalities during hyperglycemia. J Biol Chem 285: 26861–26868.
12. Matsumoto M, Pocai A, Rossetti L, Depinho RA, Accili D (2007) Impaired regulation of hepatic glucose production in mice lacking the forkhead transcription factor Foxo1 in liver. Cell Metab 6: 208–216.
13. Kitamura YI, Kitamura T, Kruse JP, Raum JC, Stein R, et al. (2005) FoxO1 protects against pancreatic beta cell failure through NeuroD and MafA induction. Cell Metab 2: 153–163.
14. Nakae J, Kitamura T, Silver DL, Accili D (2001) The forkhead transcription factor Foxo1 (Fkhr) confers insulin sensitivity onto glucose-6-phosphatase expression. J Clin Invest 108: 1359–1367.
15. Kitamura T, Nakae J, Kitamura Y, Kido Y, Biggs WH, 3rd et al. (2002) The forkhead transcription factor Foxo1 links insulin signaling to Pdx1 regulation of pancreatic beta cell growth. J Clin Invest 110: 1839–1847.
16. Paik JH, Kollipara R, Chu G, Ji H, Xiao Y, et al. (2007) FoxOs are lineage-restricted redundant tumor suppressors and regulate endothelial cell homeostasis. Cell 128: 309–323.
17. Matsumoto M, Han S, Kitamura T, Accili D (2006) Dual role of transcription factor FoxO1 in controlling hepatic insulin sensitivity and lipid metabolism. J Clin Invest 116: 2464–2472.
18. Nakae J, Kitamura T, Kitamura Y, Biggs WH, Arden KC, et al. (2003) The forkhead transcription factor foxo1 regulates adipocyte differentiation. Dev Cell 4: 119–129.
19. Guinez C, Filhoulaud G, Rayah-Benhamed F, Marmier S, Dubuquoy C, et al. (2011) O-GlcNAcylation increases ChREBP protein content and transcriptional activity in the liver. Diabetes 60: 1399–1413.
20. Horton JD, Goldstein JL, Brown MS (2002) SREBPs: activators of the complete program of cholesterol and fatty acid synthesis in the liver. J Clin Invest 109: 1125–1131.
21. Brown MS, Goldstein JL (1999) A proteolytic pathway that controls the cholesterol content of membranes, cells, and blood. Proc Natl Acad Sci U S A 96: 11041–11048.
22. Chen G, Liang G, Ou J, Goldstein JL, Brown MS (2004) Central role for liver X receptor in insulin-mediated activation of Srebp-1c transcription and stimulation of fatty acid synthesis in liver. Proc Natl Acad Sci U S A 101: 11245–11250.
23. Cha JY, Repa JJ (2007) The liver X receptor (LXR) and hepatic lipogenesis. The carbohydrate-response element-binding protein is a target gene of LXR. J Biol Chem 282: 743–751.
24. Bouche C, Serdy S, Kahn CR, Goldfine AB (2004) The cellular fate of glucose and its relevance in type 2 diabetes. Endocr Rev 25: 807–830.
25. Copeland RJ, Bullen JW, Hart GW (2008) Cross-talk between GlcNAcylation and phosphorylation: roles in insulin resistance and glucose toxicity. Am J Physiol Endocrinol Metab 295: E17–28.
26. McClain DA, Lubas WA, Cooksey RC, Hazel M, Parker GJ, et al. (2002) Altered glycan-dependent signaling induces insulin resistance and hyperleptinemia. Proc Natl Acad Sci U S A 99: 10695–10699.
27. Housley MP, Rodgers JT, Udeshi ND, Kelly TJ, Shabanowitz J, et al. (2008) O-GlcNAc regulates FoxO activation in response to glucose. J Biol Chem 283: 16283–16292.
28. Kuo M, Zilberfarb V, Gangneux N, Christeff N, Issad T (2008) O-glycosylation of FoxO1 increases its transcriptional activity towards the glucose 6-phosphatase gene. FEBS Lett 582: 829–834.
29. Housley MP, Udeshi ND, Rodgers JT, Shabanowitz J, Puigserver P, et al. (2009) A PGC-1alpha-O-GlcNAc transferase complex regulates FoxO transcription factor activity in response to glucose. J Biol Chem 284: 5148–5157.
30. Dentin R, Hedrick S, Xie J, Yates J, 3rd Montminy M (2008) Hepatic glucose sensing via the CREB coactivator CRTC2. Science 319: 1402–1405.
31. Brunet A, Bonni A, Zigmond MJ, Lin MZ, Juo P, et al. (1999) Akt promotes cell survival by phosphorylating and inhibiting a forkhead transcription factor. Cell 96: 857–868.
32. Kops GJ, de Ruiter ND, De Vries-Smits AM, Powell DR, Bos JL, et al. (1999) Direct control of the Forkhead transcription factor AFX by protein kinase B. Nature 398: 630–634.
33. Nakae J, Park BC, Accili D (1999) Insulin stimulates phosphorylation of the forkhead transcription factor FKHR on serine 253 through a Wortmannin-sensitive pathway. J Biol Chem 274: 15982–15985.
34. Nakae J, Biggs WH, Kitamura T, Cavenee WK, Wright CV, et al. (2002) Regulation of insulin action and pancreatic beta-cell function by mutated alleles of the gene encoding forkhead transcription factor Foxo1. Nat Genet 32: 245–253.
35. Spiriti J, Bogani F, van der Vaart A, Ghirlanda G (2008) Modulation of protein stability by O-glycosylation in a designed Gc-MAF analog. Biophys Chem 134: 157–167.

World Journal of Gastroenterology

Online Submissions: http://www.wjgnet.com/1007-9327office
wjg@wjgnet.com
doi:10.3748/wjg.v18.i13.1508

World J Gastroenterol 2012 April 7; 18(13): 1508-1516
ISSN 1007-9327 (print) ISSN 2219-2840 (online)

BRIEF ARTICLE

Identification of individuals with non-alcoholic fatty liver disease by the diagnostic criteria for the metabolic syndrome

Masahide Hamaguchi, Noriyuki Takeda, Takao Kojima, Akihiro Ohbora, Takahiro Kato, Hiroshi Sarui, Michiaki Fukui, Chisato Nagata, Jun Takeda

Masahide Hamaguchi, Immunology Frontier Research Center at Osaka University, Osaka 5650871, Japan
Takao Kojima, Akihiro Ohbora, Takahiro Kato, Department of Gastroenterology, Murakami Memorial Hospital, Asahi University, Gifu 5008523, Japan
Noriyuki Takeda, Hiroshi Sarui, Department of Endocrinology and Metabo lism, Murakami Memorial Hospital, Asahi University, Gifu 5008523, Japan
Michiaki Fukui, Department of Endocrinology and Metabolism, Graduate School of Medical Science, Kyoto Prefectural University of Medicine, Kyoto 6028566, Japan
Chisato Nagata, Department of Epidemiology and Preventive Medicine, Graduate School of Medicine, Gifu University, Gifu 5008523, Japan
Jun Takeda, Department of Diabetes and Endocrinology, Division of Molecule and Structure, Graduate School of Medicine, Gifu University, Gifu 5008523, Japan
Author contributions: Hamaguchi M and Takeda N designed research; Hamaguchi M, Kojima T, Takeda N, Ohbora A, Kato T, Sarui H, Fukui M, Nagata C and Takeda J performed research; Hamaguchi M analyzed data; and Hamaguchi M and Takeda N wrote the paper.
Supported by Young Scientists (B) (23790791) from Japan Society for the Promotion of Science
Correspondence to: Masahide Hamaguchi, MD, PhD, Immunology Frontier Research Center at Osaka University, Osaka 5650871, Japan. mhamaguchi@frontier.kyoto-u.ac.jp
Telephone: +81-6-68794275 Fax: +81-6-68794272
Received: June 2, 2011 Revised: January 6, 2012
Accepted: January 18, 2012
Published online: April 7, 2012

Abstract

AIM: To clarify the efficiency of the criterion of metabolic syndrome to detecting non-alcoholic fatty liver disease (NAFLD).

METHODS: Authors performed a cross-sectional study involving participants of a medical health checkup program including abdominal ultrasonography. This study involved 11 714 apparently healthy Japanese men and women, 18 to 83 years of age. NAFLD was defined by abdominal ultrasonography without an alcohol intake of more than 20 g/d, known liver disease, or current use of medication. The revised criteria of the National Cholesterol Education Program Adult Treatment Panel III were used to characterize the metabolic syndrome.

RESULTS: NAFLD was detected in 32.2% (95% CI: 31.0%-33.5%) of men (n = 1874 of 5811) and in 8.7% (95% CI: 8.0%-9.5%) of women (n = 514 of 5903). Among obese people, the prevalence of NAFLD was as high as 67.3% (95% CI: 64.8%-69.7%) in men and 45.8% (95% CI: 41.7%-50.0%) in women. Although NAFLD was thought of as being the liver phenotype of metabolic syndrome, the prevalence of the metabolic syndrome among subjects with NAFLD was low both in men and women. 66.8% of men and 70.4% of women with NAFLD were not diagnosed with the metabolic syndrome. 48.2% of men with NAFLD and 49.8% of women with NAFLD weren't overweight [body mass index (BMI) $\geq$ 25 kg/m^2]. In the same way, 68.6% of men with NAFLD and 37.9% of women with NAFLD weren't satisfied with abdominal classification ($\geq$ 90 cm for men and $\geq$ 80 cm for women). Next, authors defined it as positive at screening for NAFLD when participants satisfied at least one criterion of metabolic syndrome. The sensitivity of the definition "at least 1 criterion" was as good as 84.8% in men and 86.6% in women. Separating subjects by BMI, the sensitivity was higher in obese men and women than in non-obese men and women (92.3% *vs* 76.8% in men, 96.1% *vs* 77.0% in women, respectively).

CONCLUSION: Authors could determine NAFLD effectively in epidemiological study by modifying the usage of the criteria for metabolic syndrome.

Key words: Nonalcoholic fatty liver; Metabolic syndrome; Population based study; Methodology

Peer reviewer: Liqing Yu, Assistant Professor, Pathology-Lipid Sciences, Wake Forest University School of Medicine, Medical Center Boulevard, Winston-Salem 27157-1040, United States

Hamaguchi M, Takeda N, Kojima T, Ohbora A, Kato T, Sarui H, Fukui M, Nagata C, Takeda J. Identification of individuals with non-alcoholic fatty liver disease by the diagnostic criteria for the metabolic syndrome. *World J Gastroenterol* 2012; 18(13): 1508-1516 Available from: URL: http://www.wjgnet.com/1007-9327/full/v18/i13/1508.htm DOI: http://dx.doi.org/10.3748/wjg.v18.i13.1508

INTRODUCTION

Nonalcoholic fatty liver disease (NAFLD) is a common clinical condition with histological features that resemble those of alcohol-induced liver injury, but occurs in patients who do not drink an excessive amount of alcohol (ethanol > 20 g/d)[1,2]. This disease is often associated with obesity[3], type 2 diabetes mellitus[4,5], dyslipidemia[6], and hypertension[7]. Each of these abnormalities carries a cardiovascular disease risk, and together they are often categorized as the insulin resistance syndrome or the metabolic syndrome[8-15].

NAFLD is now considered to be the hepatic representation of the metabolic syndrome[10-15].

Conventional radiology studies used in the diagnosis of fatty liver include ultrasound (US), computed tomography, and magnetic resonance (MR) imaging. Other than these radiological studies, we have no sensitive and low invasive screening method for NAFLD. Alanine aminotransferase (ALT) > 30 IU/L was usually used as the cut off level of screening NAFLD[16,17]. This threshold had a sensitivity of 0.92 for detecting the fatty-fibrotic pattern proven by ultrasound among obese children[18]. However, ALT was within normal levels in 69% of those who had increased liver fat[19]. Similarly, in the Dallas Heart Study, 79% of the subjects with a fatty liver (liver fat content > 5.6%) had normal serum ALT[20]. This implies that a normal ALT does not exclude steatosis. Aspartate aminotransferase (AST) and gamma glutamyltransferase (GGT) also correlate with liver fat content independent of obesity[21], but are even less sensitive than serum ALT.

It was well known that NAFLD was associated with the metabolic syndrome and patients with NAFLD tend to be accompanied with the abnormal component of the metabolic syndrome. However, the efficiency of the criterion of metabolic syndrome for detecting NAFLD has not yet been clarified. We aimed to clarify the efficiency and perform a cross sectional study among apparent healthy Japanese.

MATERIALS AND METHODS

Study design

We performed a cross-sectional study involving participants of a medical health checkup program including abdominal ultrasonography. The program was conducted in the Medical Health Checkup Center at Murakami Memorial Hospital, Gifu, Japan. The purpose of the medical health checkup program is to promote public health through early detection of chronic diseases and the evaluation of their underlying risk factors. Known as a "human dock", medical services of this kind are very popular in Japan.

Study population

All the subjects participating in such health checkup programs at Murakami Memorial Hospital between January 2004 and December 2008 were invited to join this study. The study was approved by the ethics committee of Murakami Memorial Hospital.

Data collection and exclusion criteria were described previously[8]. In short, we collected the data from urinalysis, blood cell counts, blood chemistry and abdominal ultrasonography. The medical history and lifestyle factors were collected by using a self-administered questionnaire. Exclusion criteria were an alcohol intake of more than 20 g/d, known liver disease, or current use of medication which could influence the metabolic syndrome such as anti-diabetic drugs, anti-hypertensive drugs, anti-dyslipidemic drugs, anti-gout drugs, and/or anti-obesity drugs[8,10].

According to the revised National Cholesterol Education Program Adult Treatment Panel III (NCEP-ATP III)[22] or the new International Diabetes Federation (IDF) definition[23], subjects who had three or more of the following criteria were diagnosed as having the metabolic syndrome. Fatty liver was defined on the basis of ultrasonographic findings[24]. Of 4 known criteria (hepatorenal echo contrast, liver brightness, deep attenuation, and vascular blurring), the participants were required to have hepatorenal contrast and liver brightness to be given a diagnosis of fatty liver[24].

During study period, we invited 20 012 participants in the health checkup program to enroll in the study. Of those, a total of 17 262 Japanese participants (10 329 men and 6933 women) were enrolled after giving informed consent to be included in the study. We excluded 621 participants (420 men and 201 women) who had known liver disease. In addition, 3330 participants (3042 men and 288 women) who consumed more than 20 g of ethanol per day and 1579 participants (1056 men and 541 women) who were currently receiving medication were excluded. As a result, this study ultimately consisted of 11 714 participants (5811 men and 5903 women). The mean ± SD age was 45.5 ± 9.4 years (range: 18 years to 83 years) for men and 44.3 ± 9.3 years (range: 18 years to 79 years) for women, respectively. The mean body mass index (BMI) was 23.2 ± 3.1 kg/m^2 (range: 14.3 to 41.0 kg/m^2) in men and 21.1 ± 3.0 kg/m^2 (range: 14.0 to 58.3 kg/m^2) in women, respectively. The mean abdominal circumference was 81.2 ± 8.1 cm (range: 57.3 cm to 127.5 cm) in men and 71.4 ± 8.2 cm (range: 49.0 cm to 145.0 cm) in women, respectively.

Table 1 The basic characteristics of the study population and the association of nonalcoholic fatty liver disease with gender difference

Men	Total *n* (%)	Obese *n* (%)	Non-obese *n* (%)
Number	5811	1441	4370
NAFLD	1874 (32.2)	970 (67.3)	904 (20.7%)
5 criteria of the metabolic syndrome			
Increased abdominal circumference	791 (13.6)	703 (48.8)	88 (2)
Elevated fasting glucose level	1967 (33.8)	704 (48.9)	1263 (28.9)
Elevated blood pressure	1294 (22.3)	575 (39.9)	719 (16.5)
Decreased HDL cholesterol level	1736 (29.9)	654 (45.4)	1082 (24.8)
Elevated triglyceride level	1063 (18.3)	484 (33.6)	579 (13.2)
ALT > 30	1269 (21.8)	670 (46.5)	599 (13.7)
MS defined by rNCEP-ATP Ⅲ	873 (15)	578 (40.1)	295 (6.8)
MS defined by IDF	479 (8.2)	443 (30.7)	36 (0.8)
At least 1 criterion	3680 (63.3)	1291 (89.6)	2389 (54.7)
At least 2 criteria	1955 (33.6)	957 (66.4)	998 (22.8)
At least 1 criterion or ALT > 30 IU/L	3885 (66.9)	1337 (92.8)	2548 (58.3)
Women			
Number	5903	563	5340
NAFLD	514 (8.7)	258 (45.8)	256 (4.8)
5 criteria of the metabolic syndrome			
Increased abdominal circumference	878 (14.9)	430 (76.4)	448 (8.4)
Elevated fasting glucose level	679 (11.5)	176 (31.3)	503 (9.4)
Elevated blood pressure	578 (9.8)	185 (32.9)	393 (7.4)
Decreased HDL cholesterol level	1320 (22.4)	265 (47.1)	1055 (19.8)
Elevated triglyceride level	195 (3.3)	73 (13)	122 (2.3)
Elevated ALT (ALT > 30 IU/L)	200 (3.4)	78 (13.9)	122 (2.3)
MS defined by rNCEP-ATP Ⅲ	300 (5.1)	174 (30.9)	126 (2.4)
MS defined by IDF	254 (4.3)	162 (28.8)	92 (1.7)
At least 1 criterion	2374 (40.2)	511 (90.8)	1863 (34.9)
At least 2 criteria	853 (14.5)	355 (63.1)	498 (9.3)
At least 1 criterion or elevated ALT	2430 (41.2)	515 (91.5)	1915 (35.9)

NAFLD: Nonalcoholic fatty liver disease; US: Abdominal ultrasonography; BMI: Body mass index; HDL: High density lipoprotein; MS: Metabolic syndrome; rNCEP-ATPⅢ: Revised National Cholesterol Education Program Adult Treatment Panel Ⅲ definition; IDF: International diabetes federation definition; ALT: Alanine aminotransferase.

Statistical analysis

The R version 2.9.0 (available from http://www.r-project.org/) was used for statistical analyses. Two groups of subjects were compared by using the unpaired *t*-test and the chi-square test, and a $P < 0.05$ was accepted as a significant level.

RESULTS

Basic characteristics of study population

The metabolic syndrome defined by revised NCEP-ATPⅢ definition was detected in 15.0% (95% CI: 14.1%-16.0%) of men ($n = 873$ of 5811) and in 5.1% (95% CI: 4.5%-5.7%) of women ($n = 300$ of 5903). The metabolic syndrome defined by IDF definition was detected in 8.2% (95% CI: 7.5%-9.0%) of men ($n = 479$ of 5811) and in 4.3% (95% CI: 3.8%-4.8%) of women ($n = 254$ of 5903) (Table 1). Among obese people, the metabolic syndrome defined by revised NCEP-ATPⅢ definition was detected in 40.1% (95% CI: 37.6%-42.7%) of men and in 30.9% (95% CI: 27.1%-34.9%) of women, and the metabolic syndrome defined by IDF definition was detected in 30.7% (95% CI: 28.4%-33.2%) of men and in 28.8% (95% CI: 25.1%-32.7%) of women, respectively (Table 1).

Association of NAFLD with gender difference, or body fat accumulation

NAFLD was detected in 32.2% (95% CI: 31.0%-33.5%) of men ($n = 1874$ of 5811) and in 8.7% (95% CI: 8.0%-9.5%) of women ($n = 514$ of 5903). The prevalence of NAFLD in men was four times higher than those in women (Table 1). Among obese people, the prevalence of NAFLD was as high as 67.3% (95% CI: 64.8%-69.7%) in men and 45.8% (95% CI: 41.7%-50.0%) in women (Table 1). NAFLD was associated with body fat accumulation strongly both in men and women.

When we separated by quartile the subjects according to their BMI or abdominal circumference, half of NAFLD men and three quarters of NAFLD women were classified in the superior quartile. The prevalence of NAFLD was increased according to the increase of BMI or abdominal circumference (Figure 1A). The role of BMI for NAFLD was equal to that of abdominal circumference both in men and women. The ratio of NAFLD in the superior quartile/total NAFLD was higher in women than in men. The prevalence of individuals who met two or more of the MS criteria other than waist circumference was increased according to the increase of BMI or abdominal circumference (Figure 1B).

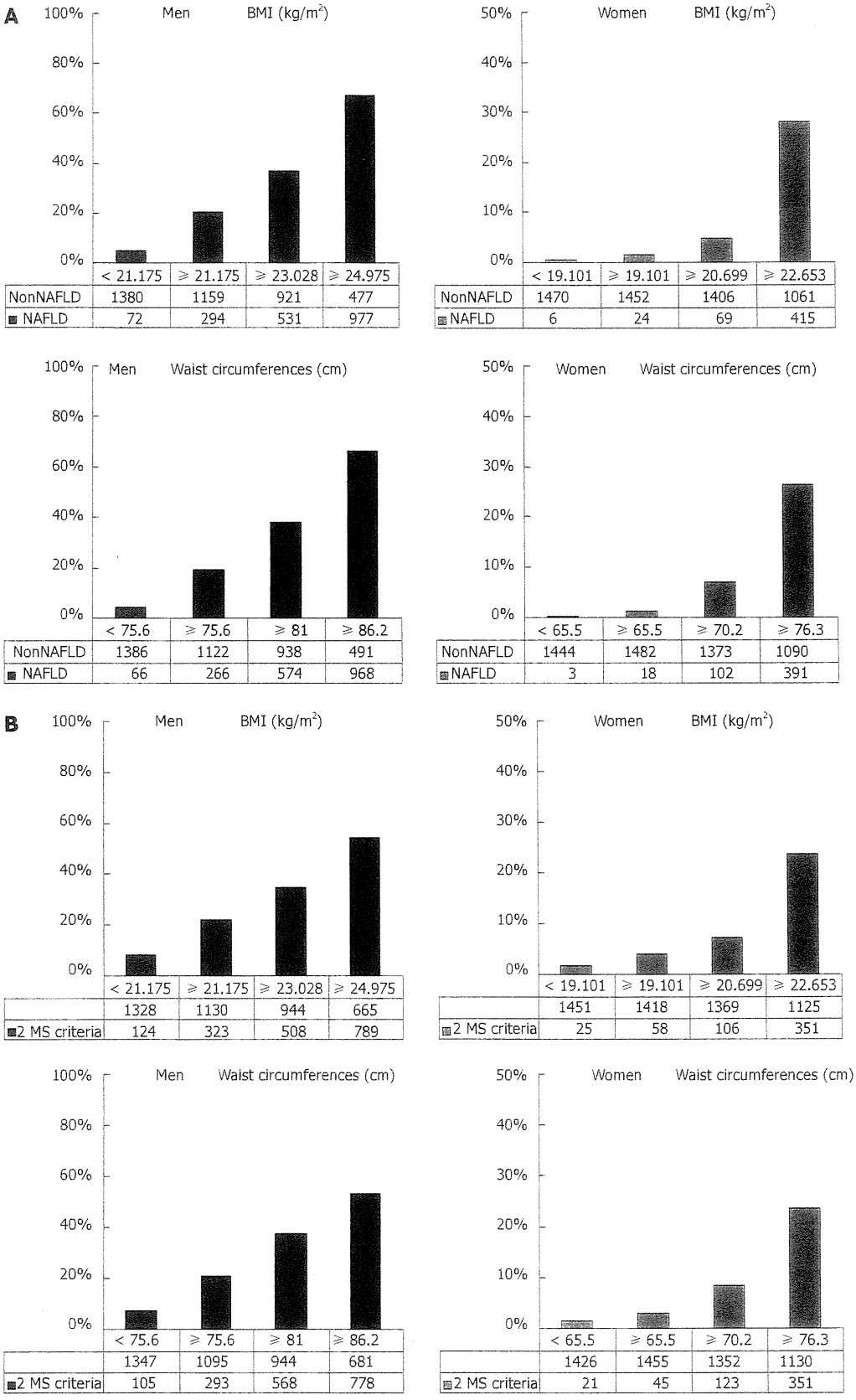

Figure 1 We separated the subjects by quartile according to their body mass index or abdominal circumference. A: The bar indicated the prevalence (%) of individuals with NAFLD; B: Individuals who meet two or more of the MS criteria other than waist circumference according to BMI or waist circumference quartiles. 2 MS criteria means individuals who meets two or more of the MS criteria other than waist circumference. NAFLD: Nonalcoholic fatty liver disease; BMI: Body mass index; MS: Metabolic syndrome.

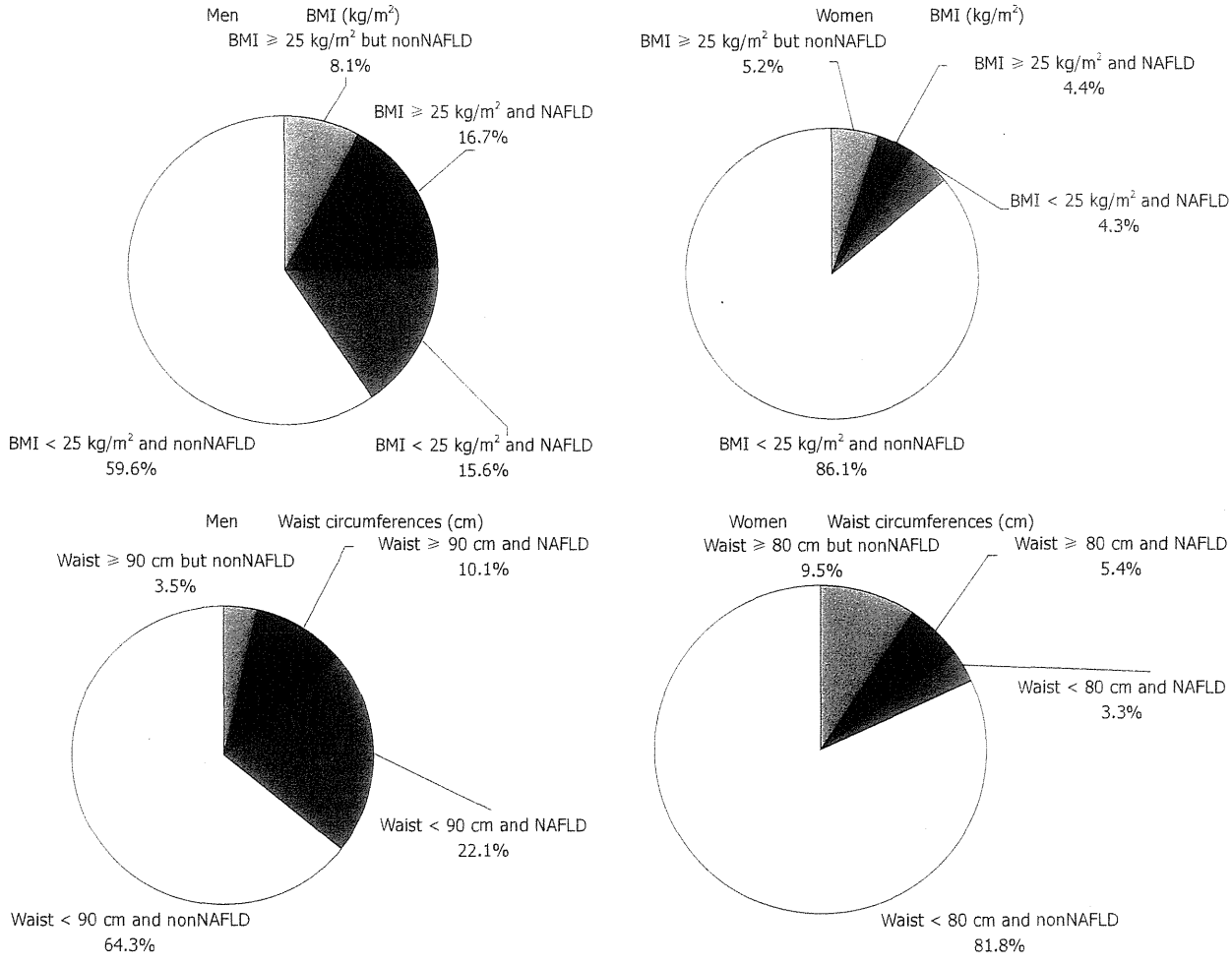

Figure 2 This figure indicates the prevalence of non-alcoholic fatty liver disease and alcoholic fatty liver disease with or without patients being overweight (BMI ≥ 25 kg/m²) or having elevated abdominal circumferences (≥ 90 cm for men and ≥ 80 cm for women). Data was expressed as prevalence (%). NAFLD accompanied with being overweight occurred in 51.8% of NAFLD men (970/1874) and 50.2% of NAFLD women (258/514). NAFLD accompanied by elevated abdominal circumference occurred in 31.4% of NAFLD men (588/1874) and 62.1% of women (319/514). NAFLD: Non-alcoholic fatty liver disease; BMI: Body mass index.

Role of the criteria of the metabolic syndrome in detecting or diagnosing NAFLD in obese or non-obese population

Although NAFLD was associated with obesity or body fat accumulation strongly, the population that was neither overweight (BMI ≥ 25 kg/m²) nor had elevated abdominal circumference was not small (Figure 2). Actually, 48.2% of men with NAFLD and 49.8% of women with NAFLD were not overweight (BMI ≥ 25 kg/m²). Similarly, 68.6% of men with NAFLD and 37.9% of women with NAFLD did not satisfy increased abdominal circumference classification. Half of the NAFLD group was classified as non-obese, but the prevalence of NAFLD among the non-obese population was lower. These facts means an effective method is needed to detect NAFLD among the non-obese population. Then, we separated the subjects into two groups, obese group or non-obese group, and investigated the efficacy of the criteria of metabolic syndrome for detecting NAFLD in each group.

Among the criteria for metabolic syndrome, the criterion of abdominal circumferences (≥ 80 cm) had high sensitivity (87.6%) for detecting NAFLD in women who were overweight (BMI ≥ 25 kg/m²) (Table 2). In other words, abdominal circumference was effective for detecting NAFLD in obese women. However, the criterion of abdominal circumference had low sensitivity (36.3%) in non-obese women. The sensitivity of abdominal circumference (≥ 90 cm) was very low (5.8%) in non-obese men. Even in obese men the sensitivity was not high (55.3%). Other criteria for metabolic syndrome had higher sensitivity in obese men and women than in the non-obese population but sensitivity never exceeded 60%.

As a screening tool for NAFLD, the sensitivity of elevated ALT (ALT > 30 IU/L) was 49.7% in men, which exceeded the sensitivity of the criteria of metabolic syndrome, but it was 17.7% in women, which was lower than all metabolic syndrome criteria were. On the other hand, the specificity of elevated ALT was as high as 90.6% in men and 98.0% in women, but the criteria of metabolic syndrome had equally high specificity.

Next, we defined it as positive at screening for NAFLD

Table 2 The role of the criteria of the metabolic syndrome in detecting or diagnosing nonalcoholic fatty liver disease in obese or non-obese population

	Men				Women			
Sensitivity	Total %	Obese %	Non-obese %	*P* value	Total %	Obese %	Non-obese %	*P* value
5 criteria of the metabolic syndrome								
Increased abdominal circumference	31.40	55.30	5.80	< 0.001	62.10	87.60	36.30	< 0.001
Elevated fasting glucose level	49.10	52.10	45.90	0.008	36.80	42.20	31.30	0.013
Elevated blood pressure	34.70	44.10	24.60	< 0.001	31.90	41.50	22.30	< 0.001
Decreased HDL cholesterol level	44.10	49.10	38.80	< 0.001	50.40	56.60	44.10	0.006
Elevated triglyceride level	35.20	41.00	28.90	< 0.001	17.90	20.50	15.20	0.15
Elevated ALT (ALT > 30 IU/L)	47.90	59.20	35.80	< 0.001	17.70	24.00	11.30	< 0.001
MS defined by rNCEP-ATP Ⅲ	33.20	48.60	16.80	< 0.001	32.50	45.00	19.90	< 0.001
MS defined by IDF	21.00	38.10	2.70	< 0.001	29.60	43.40	15.60	< 0.001
At least 1 criterion	84.80	92.30	76.80	< 0.001	86.60	96.10	77.00	< 0.001
At least 2 criteria	61.00	74.20	46.90	< 0.001	61.10	77.50	44.50	< 0.001
At least 1 criterion or elevated ALT	90.40	96.20	84.20	< 0.001	87.40	96.90	79.70	< 0.001
Specificity								
5 criteria of the metabolic syndrome								
Increased abdominal circumference	94.80	64.50	99.00	< 0.001	89.60	33.10	93.00	< 0.001
Elevated fasting glucose level	73.40	57.70	75.50	< 0.001	90.90	78.00	91.70	< 0.001
Elevated blood pressure	83.60	68.80	85.70	< 0.001	92.30	74.40	93.40	< 0.001
Decreased HDL cholesterol level	76.90	62.20	78.90	< 0.001	80.30	61.00	81.50	< 0.001
Elevated triglyceride level	89.70	81.70	90.80	< 0.001	98.10	93.40	98.40	< 0.001
Elevated ALT (ALT > 30 IU/L)	90.60	79.60	92.10	< 0.001	98.00	94.80	98.20	< 0.001
MS defined by rNCEP-ATP Ⅲ	93.60	77.30	95.90	< 0.001	97.50	81.00	98.50	< 0.001
MS defined by IDF	97.80	84.50	99.70	< 0.001	98.10	83.60	99.00	< 0.001
At least 1 criterion	46.90	15.90	51.10	< 0.001	64.20	13.80	67.20	< 0.001
At least 2 criteria	79.40	49.70	83.40	< 0.001	90.00	49.20	92.40	< 0.001
At least 1 criterion or elevated ALT	44.30	14.20	48.40	< 0.001	63.20	13.10	65.40	< 0.001

NAFLD: Nonalcoholic fatty liver disease; US: Abdominal ultrasonography; BMI: Body mass index; HDL: High dense lipoprotein; MS: Metabolic syndrome; rNCEP-ATPⅢ: Revised National Cholesterol Education Program Adult Treatment Panel Ⅲ definition; IDF: International Diabetes Federation definition; ALT: Alanine aminotransferase.

when participants satisfied at least one or two components of metabolic syndrome. The sensitivity of the definition "at least 1 criterion" was 84.8% in men and 86.6% in women. Separating subjects with BMI, the sensitivity was higher in obese men and women than in non-obese men and women (92.3% *vs* 76.8% in men, 96.1% *vs* 77.0% in women, respectively).

The prevalence of subjects with NAFLD who also had the metabolic syndrome is indicated in Figure 3. Although NAFLD was thought of as being the liver phenotype of metabolic syndrome, the prevalence of the metabolic syndrome among subjects with NAFLD was low both in men and women. Among men with NAFLD, 66.8% were not diagnosed with the metabolic syndrome defined by revised NCEP-ATPⅢ definition, and 79.0% were not diagnosed with the metabolic syndrome as defined by revised IDF definition. Even in women, 70.4% and 67.5%, respectively, were not diagnosed withmetabolic syndrome by revised NCEP-ATPⅢ definition and revised IDF definition. These results mean that a large number of participants diagnosed with the metabolic syndrome have NAFLD, but a large number of participants with NAFLD were not diagnosed with the metabolic syndrome, whether we used revised NECP-ATPⅢ criteria or IDF criteria.

DISCUSSION

In this study, we clarified the impact of the criteria of the metabolic syndrome for diagnosing NAFLD in a healthy population. The metabolic syndrome was associated with abdominal obesity and its criteria include waist circumference[22,23,25,26], and NAFLD was reported to be associated with abdominal obesity. However, our results indicated there was no significant difference between BMI and waist circumferences as the strength of association with NAFLD or the accumulation of metabolic syndrome criteria.

The presence of multiple metabolic disorders such as diabetes mellitus, obesity, dyslipidaemia and hypertension is associated with a potentially progressive, severe liver disease[15,27]. Previous reports demonstrated that prevalence of NAFLD increased to 10%-80% in individuals with obesity, 35%-90% in individuals with type 2 diabetes mellitus, 30%-56% in individuals with hypertension, and 26%-58% in individuals with dyslipidemia[9,28-30]. Another study in a Japanese population showed that prevalence of NAFLD increased to 43% in individuals with impaired fasting glucose and 62% in individuals with type 2 diabetes mellitus[28]. Some studies estimate the prevalence of NAFLD be up to 15%-30% of the general population[8,31,32], and the prevalence of metabolic syndrome was estimated to be up to 25% of the general population[33]. In those patients with the metabolic syndrome, liver fat content is significantly increased up to 4-fold higher than those without the metabolic syndrome[34], and the incidence of NAFLD has been shown to be increased 4-fold in men and 11-fold in women with the metabolic syndrome[8].

Our data clearly indicated that 21% to 33% of sub-

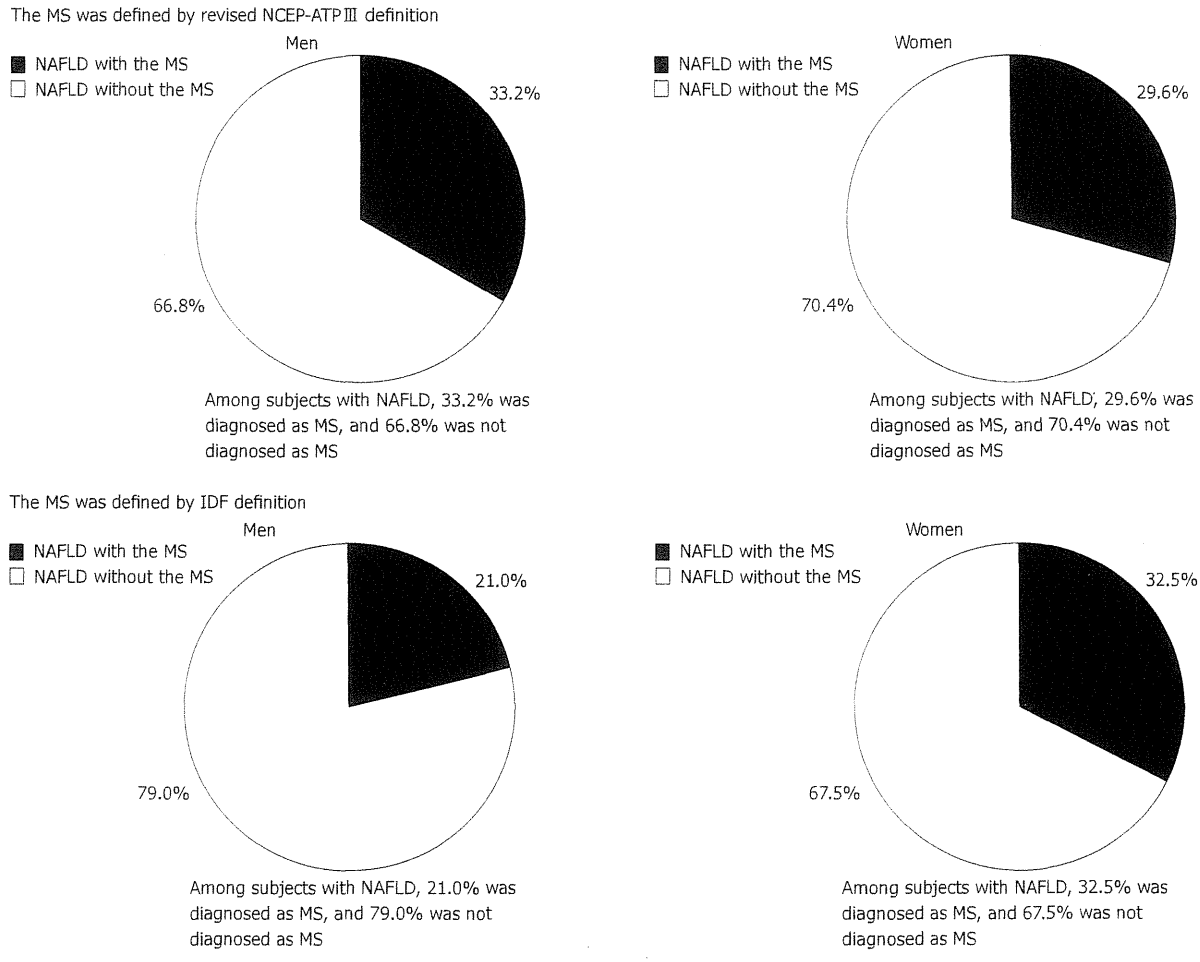

Figure 3 The prevalence of subjects with or without the metabolic syndrome among 1874 men and 514 women with non-alcoholic fatty liver disease. Data was expressed as prevalence (%). The metabolic syndrome (MS) was diagnosed using revised IDF. Among men with NAFLD, 66.8% and 79.0% were not diagnosed with the MS defined by revised NCEP-ATPⅢ definition and revised IDF definition, respectively. In women, 70.4% and 67.5%, respectively, were not diagnosed with the MS by revised NCEP-ATPⅢ definition and revised IDF definition. IDF: International Diabetes Federation; NCEP-ATPⅢ: National Cholesterol Education Program Adult Treatment Panel Ⅲ; NAFLD: Non-alcoholic fatty liver disease.

jects with NAFLD, depending on gender and the criteria used, were diagnosed with the metabolic syndrome. Several previous studies reported how many subjects with NAFLD were diagnosed with the metabolic syndrome, but almost all previous studies were hospital studies. Three population based studies mentioned the prevalence of subjects with NAFLD who were diagnosed with the metabolic syndrome among the general population[8,35,36]. In these studies, the prevalence of the metabolic syndrome among subjects with NAFLD was 17% to 36% depending on gender and the criteria used. The reported prevalence was similar to ours.

There has been no report regarding the sensitivity and specificity of the metabolic syndrome for detecting NAFLD. Among the criteria for metabolic syndrome, the criterion of abdominal circumference had high sensitivity in obese women. However, it had low sensitivity (36.3%) in non-obese women and was very low (5.8%) in non-obese men and low (55.3% in obese men. Other than the criterion of abdominal circumference, none of the sensitivities exceeded 60%. In our study, the specificity of elevated ALT (ALT > 30 IU/L) was 90.6% in men and 98.0% in women. However, the sensitivity was as low as 47.9% in men and 17.7% in women. The specificity of elevated ALT was significantly higher among obese subjects than among non-obese subjects, and sensitivity was higher among obese subjects than among non-obese subjects.

When we investigated the predictability of each component of metabolic syndrome such as abdominal circumference, fasting blood sugar, serum lipid, and blood pressure, each component had high specificity but low sensitivity, similar to elevated ALT. Therefore, we defined it as screening positive for NAFLD, when subjects satisfied at least one criterion of metabolic syndrome; the sensitivity was 84.8% in men and 86.6% in women. Additionally, we defined it as positive when subjects satisfied at least one criterion of metabolic syndrome or elevated ALT. The sensitivity of "at least 1 criterion or elevated ALT" was 90.4% in men and 87.4% in women. However, the specificity of "at least 1 criterion or elevated ALT" was lower -44%-63%.

The result of our study means that we could identify NAFLD effectively in epidemiological study by modifying the usage of the criteria for metabolic syndrome. It is clinically critical evidence that a large part of patients with NAFLD were not diagnosed with the metabolic syndrome, when we used today's definition for the metabolic syndrome. However, our subject population consisted only of Japanese, thus, the generalizability of our study to non-Japanese populations is uncertain. It is one of our study limitations that we used abdominal ultrasonography for diagnosing NAFLD, although the validation ultrasonography had a sensitivity of 91.7% and a specificity of 100%[24].

COMMENTS

Background

It is well known that non-alcoholic fatty liver disease (NAFLD) is associated with the metabolic syndrome and patients with NAFLD tend to also have the metabolic syndrome.

Research frontiers

The impact of overlap between NAFLD and the metabolic syndrome has not been evaluated yet.

Innovations and breakthroughs

It is clinically critical evidence that a large number of patients with NAFLD were not diagnosed with the metabolic syndrome in a healthy Japanese population.

Applications

The authors could identify NAFLD effectively by modifying the usage of the criteria for metabolic syndrome.

Peer review

It is a relatively large population study. The conclusion is consistent with recent observations showing the dissociation between NAFLD and other parameters of metabolic syndrome. The readers of this journal will be interested in the findings of this study.

REFERENCES

1 **Brunt EM**, Janney CG, Di Bisceglie AM, Neuschwander-Tetri BA, Bacon BR. Nonalcoholic steatohepatitis: a proposal for grading and staging the histological lesions. *Am J Gastroenterol* 1999; **94**: 2467-2474

2 **Mulhall BP**, Ong JP, Younossi ZM. Non-alcoholic fatty liver disease: an overview. *J Gastroenterol Hepatol* 2002; **17**: 1136-1143

3 **Bellentani S**, Saccoccio G, Masutti F, Crocè LS, Brandi G, Sasso F, Cristanini G, Tiribelli C. Prevalence of and risk factors for hepatic steatosis in Northern Italy. *Ann Intern Med* 2000; **132**: 112-117

4 **Akbar DH**, Kawther AH. Nonalcoholic fatty liver disease in Saudi type 2 diabetic subjects attending a medical outpatient clinic: prevalence and general characteristics. *Diabetes Care* 2003; **26**: 3351-3352

5 **Gupte P**, Amarapurkar D, Agal S, Baijal R, Kulshrestha P, Pramanik S, Patel N, Madan A, Amarapurkar A. Non-alcoholic steatohepatitis in type 2 diabetes mellitus. *J Gastroenterol Hepatol* 2004; **19**: 854-858

6 **Assy N**, Kaita K, Mymin D, Levy C, Rosser B, Minuk G. Fatty infiltration of liver in hyperlipidemic patients. *Dig Dis Sci* 2000; **45**: 1929-1934

7 **Donati G**, Stagni B, Piscaglia F, Venturoli N, Morselli-Labate AM, Rasciti L, Bolondi L. Increased prevalence of fatty liver in arterial hypertensive patients with normal liver enzymes: role of insulin resistance. *Gut* 2004; **53**: 1020-1023

8 **Hamaguchi M**, Kojima T, Takeda N, Nakagawa T, Taniguchi H, Fujii K, Omatsu T, Nakajima T, Sarui H, Shimazaki M, Kato T, Okuda J, Ida K. The metabolic syndrome as a predictor of nonalcoholic fatty liver disease. *Ann Intern Med* 2005; **143**: 722-728

9 **Radu C**, Grigorescu M, Crisan D, Lupsor M, Constantin D, Dina L. Prevalence and associated risk factors of non-alcoholic fatty liver disease in hospitalized patients. *J Gastrointestin Liver Dis* 2008; **17**: 255-260

10 **McCullough AJ**. The clinical features, diagnosis and natural history of nonalcoholic fatty liver disease. *Clin Liver Dis* 2004; **8**: 521-533, viii

11 **Adams LA**, Angulo P. Recent concepts in non-alcoholic fatty liver disease. *Diabet Med* 2005; **22**: 1129-1133

12 **Marchesini G**, Marzocchi R, Agostini F, Bugianesi E. Nonalcoholic fatty liver disease and the metabolic syndrome. *Curr Opin Lipidol* 2005; **16**: 421-427

13 **Neuschwander-Tetri BA**. Nonalcoholic steatohepatitis and the metabolic syndrome. *Am J Med Sci* 2005; **330**: 326-335

14 **Lavine JE**, Schwimmer JB. Nonalcoholic fatty liver disease in the pediatric population. *Clin Liver Dis* 2004; **8**: 549-558, viii-ix

15 **Marchesini G**, Bugianesi E, Forlani G, Cerrelli F, Lenzi M, Manini R, Natale S, Vanni E, Villanova N, Melchionda N, Rizzetto M. Nonalcoholic fatty liver, steatohepatitis, and the metabolic syndrome. *Hepatology* 2003; **37**: 917-923

16 **Fraser A**, Longnecker MP, Lawlor DA. Prevalence of elevated alanine aminotransferase among US adolescents and associated factors: NHANES 1999-2004. *Gastroenterology* 2007; **133**: 1814-1820

17 **Strauss RS**, Barlow SE, Dietz WH. Prevalence of abnormal serum aminotransferase values in overweight and obese adolescents. *J Pediatr* 2000; **136**: 727-733

18 **Tazawa Y**, Noguchi H, Nishinomiya F, Takada G. Serum alanine aminotransferase activity in obese children. *Acta Paediatr* 1997; **86**: 238-241

19 **Szczepaniak LS**, Nurenberg P, Leonard D, Browning JD, Reingold JS, Grundy S, Hobbs HH, Dobbins RL. Magnetic resonance spectroscopy to measure hepatic triglyceride content: prevalence of hepatic steatosis in the general population. *Am J Physiol Endocrinol Metab* 2005; **288**: E462-E468

20 **Browning JD**, Szczepaniak LS, Dobbins R, Nuremberg P, Horton JD, Cohen JC, Grundy SM, Hobbs HH. Prevalence of hepatic steatosis in an urban population in the United States: impact of ethnicity. *Hepatology* 2004; **40**: 1387-1395

21 **Thamer C**, Tschritter O, Haap M, Shirkavand F, Machann J, Fritsche A, Schick F, Häring H, Stumvoll M. Elevated serum GGT concentrations predict reduced insulin sensitivity and increased intrahepatic lipids. *Horm Metab Res* 2005; **37**: 246-251

22 **Expert Panel on Detection, Evaluation, and Treatment of High Blood Cholesterol in Adults**. Executive Summary of The Third Report of The National Cholesterol Education Program (NCEP) Expert Panel on Detection, Evaluation, And Treatment of High Blood Cholesterol In Adults (Adult Treatment Panel III). *JAMA* 2001; **285**: 2486-2497

23 **Alberti KG**, Zimmet P, Shaw J. Metabolic syndrome--a new world-wide definition. A Consensus Statement from the International Diabetes Federation. *Diabet Med* 2006; **23**: 469-480

24 **Hamaguchi M**, Kojima T, Itoh Y, Harano Y, Fujii K, Nakajima T, Kato T, Takeda N, Okuda J, Ida K, Kawahito Y, Yoshikawa T, Okanoue T. The severity of ultrasonographic findings in nonalcoholic fatty liver disease reflects the metabolic syndrome and visceral fat accumulation. *Am J Gastroenterol* 2007; **102**: 2708-2715

25 **Stone NJ**, Bilek S, Rosenbaum S. Recent National Cholesterol Education Program Adult Treatment Panel III update: adjustments and options. *Am J Cardiol* 2005; **96**: 53E-59E

26 **World Health Organization Western Pacific Region, International Association for the Study of Obesity, International Obesity Task Force.** The Asia-Pacific Perspective: Redefining Obesity and Its Treatment. Sydney: Health Com-

munications, 2000
27 **Marchesini G**, Marzocchi R. Metabolic syndrome and NASH. *Clin Liver Dis* 2007; **11**: 105-117, ix
28 **Jimba S**, Nakagami T, Takahashi M, Wakamatsu T, Hirota Y, Iwamoto Y, Wasada T. Prevalence of non-alcoholic fatty liver disease and its association with impaired glucose metabolism in Japanese adults. *Diabet Med* 2005; **22**: 1141-1145
29 **Fan JG**, Zhu J, Li XJ, Chen L, Lu YS, Li L, Dai F, Li F, Chen SY. Fatty liver and the metabolic syndrome among Shanghai adults. *J Gastroenterol Hepatol* 2005; **20**: 1825-1832
30 **Amarapurkar DN**, Hashimoto E, Lesmana LA, Sollano JD, Chen PJ, Goh KL. How common is non-alcoholic fatty liver disease in the Asia-Pacific region and are there local differences? *J Gastroenterol Hepatol* 2007; **22**: 788-793
31 **Neuschwander-Tetri BA**, Caldwell SH. Nonalcoholic steatohepatitis: summary of an AASLD Single Topic Conference. *Hepatology* 2003; **37**: 1202-1219
32 **Bedogni G**, Miglioli L, Masutti F, Tiribelli C, Marchesini G, Bellentani S. Prevalence of and risk factors for nonalcoholic fatty liver disease: the Dionysos nutrition and liver study. *Hepatology* 2005; **42**: 44-52
33 **Ford ES**, Giles WH, Dietz WH. Prevalence of the metabolic syndrome among US adults: findings from the third National Health and Nutrition Examination Survey. *JAMA* 2002; **287**: 356-359
34 **Kotronen A**, Westerbacka J, Bergholm R, Pietiläinen KH, Yki-Järvinen H. Liver fat in the metabolic syndrome. *J Clin Endocrinol Metab* 2007; **92**: 3490-3497
35 **Sung KC**, Ryan MC, Wilson AM. The severity of nonalcoholic fatty liver disease is associated with increased cardiovascular risk in a large cohort of non-obese Asian subjects. *Atherosclerosis* 2009; **203**: 581-586
36 **Karnikowski M**, Córdova C, Oliveira RJ, Karnikowski MG, Nóbrega Ode T. Non-alcoholic fatty liver disease and metabolic syndrome in Brazilian middle-aged and older adults. *Sao Paulo Med J* 2007; **125**: 333-337

S- Editor Gou SX **L- Editor** O'Neill M **E- Editor** Zhang DN

THE JOURNAL OF BIOLOGICAL CHEMISTRY VOL. 287, NO. 27, pp. 23236–23245, June 29, 2012
Published in the U.S.A.

Anks4b, a Novel Target of HNF4α Protein, Interacts with GRP78 Protein and Regulates Endoplasmic Reticulum Stress-induced Apoptosis in Pancreatic β-Cells*[S]

Received for publication, April 3, 2012, and in revised form, May 11, 2012 Published, JBC Papers in Press, May 15, 2012, DOI 10.1074/jbc.M112.368779

Yoshifumi Sato[‡1], Mitsutoki Hatta[‡1], Md. Fazlul Karim[‡1,2], Tomohiro Sawa[§¶], Fan-Yan Wei[‖], Shoki Sato[‡], Mark A. Magnuson[**], Frank J. Gonzalez[‡‡], Kazuhito Tomizawa[‖], Takaaki Akaike[§], Tatsuya Yoshizawa[‡], and Kazuya Yamagata[‡3]

From the Departments of [‡]Medical Biochemistry and [§]Microbiology, Faculty of Life Sciences, Kumamoto University, Kumamoto 860-8556, Japan, [¶]PRESTO, Japan Science and Technology Agency (JST), 4-1-8 Honcho Kawaguchi, Saitama 332-001, Japan, the [‖]Department of Molecular Physiology, Faculty of Life Sciences, Kumamoto University, Kumamoto, Japan the [**]Department of Molecular Physiology and Biophysics, Vanderbilt University School of Medicine, Nashville, Tennessee 37232, and the [‡‡]Laboratory of Metabolism, NCI, National Institutes of Health, Bethesda, Maryland 20814

Background: Target genes of HNF4α in β-cells are largely unknown.
Results: Expression of Anks4b is decreased in the βHNF4α KO islets. HNF4α activates Anks4b promoter activity. Anks4b binds to GRP78 and regulates sensitivity to ER stress.
Conclusion: HNF4α novel target gene, *Anks4b*, regulates the susceptibility of β-cells to ER stress.
Significance: Anks4b is a novel molecule involved in ER stress.

Mutations of the *HNF4A* gene cause a form of maturity-onset diabetes of the young (MODY1) that is characterized by impairment of pancreatic β-cell function. HNF4α is a transcription factor belonging to the nuclear receptor superfamily (NR2A1), but its target genes in pancreatic β-cells are largely unknown. Here, we report that ankyrin repeat and sterile α motif domain containing 4b (Anks4b) is a target of HNF4α in pancreatic β-cells. Expression of Anks4b was decreased in both βHNF4α KO islets and HNF4α knockdown MIN6 β-cells, and HNF4α activated Anks4b promoter activity. Anks4b bound to glucose-regulated protein 78 (GRP78), a major endoplasmic reticulum (ER) chaperone protein, and overexpression of Anks4b enhanced the ER stress response and ER stress-associated apoptosis of MIN6 cells. Conversely, suppression of Anks4b reduced β-cell susceptibility to ER stress-induced apoptosis. These results indicate that Anks4b is a HNF4α target gene that regulates ER stress in β-cells by interacting with GRP78, thus suggesting that HNF4α is involved in maintenance of the ER.

Hepatocyte nuclear factor (HNF)[4] 4α, a transcription factor belonging to the nuclear receptor superfamily (NR2A1), is expressed in the liver, pancreas, kidney, and intestine (1, 2). HNF4α has multiple functional domains, including the N-terminal A/B domain associated with the transactivation domain (AF-1), a DNA binding C domain, a functionally complex E domain that forms a ligand binding domain, a dimerization interface and transactivation domain (AF-2), and an F domain with a negative regulatory function (3, 4). HNF4α predominantly binds to a 6-bp repeat (AGGTCA) with a 1-bp spacer (mainly A) called direct repeat (DR1).

Maturity-onset diabetes of the young (MODY) is a genetically heterogeneous monogenic disorder that accounts for 2–5% of type 2 diabetes (5). We discovered that mutations of the human *HNF4A* gene cause a particular form of MODY known as MODY1 (6). The primary pathogenesis of MODY1 involves dysfunction of pancreatic β-cells (5). In addition, it has been shown that targeted disruption of HNF4α in pancreatic β-cells leads to defective insulin secretion in mice (7, 8). These findings have demonstrated that HNF4α has an important role in β-cells.

In the liver, HNF4α plays a critical role in nutrient transport and metabolism by regulating numerous target genes, including phosphoenolpyruvate carboxykinase (*PCK1*), glucose-6-phosphatase (*G6PC*), apolipoprotein AII (*APOA2*), and microsomal triglyceride transfer protein (*MTTP*) (9, 10). In contrast, we have little information about the target genes of HNF4α in pancreatic β-cells. Previous *in vitro* studies have suggested that

* This work was supported by a grant-in-aid for scientific research (B), a grant-in-aid for scientific research (S), a grant-in-aid for scientific research in innovative areas, a grant from the Ministry of Health Labour and Welfare, a grant from Takeda Science Foundation, a grant from Novo Nordisk Insulin Research Foundation, a grant from Banyu Life Science Foundation International, and a grant from Japan Diabetes Foundation.

[S] This article contains supplemental Tables 1 and 2 and supplemental Figs. 1–8.

[1] *These authors contributed equally to this work.*

[2] Supported by a scholarship from the International Priority Graduate Programs Advanced Graduate Courses for International Students, Ministry of Education, Culture, Sports, Science, and Technology in Japan.

[3] To whom correspondence should be addressed. Fax: 81-96-364-6940; E-mail: k-yamaga@kumamoto-u.ac.jp.

[4] The abbreviations used are: HNF, hepatocyte nuclear factor; MODY, Maturity-onset diabetes of the young; ER, endoplasmic reticulum; Anks4b, ankyrin repeat and sterile α motif domain containing 4b; TG, thapsigargin; CHOP, C/EBP homologous protein; C/EBP, CCAAT-enhancer-binding protein; BiP, binding immunoglobulin protein; ESI-Q-TOF, electrospray mass ionization-quadrupole-time-of-flight; KD, knockdown; FL, full-length; MUT, mutant.

HNF4α regulates the expression of pancreatic β-cell genes involved in glucose metabolism, such as insulin (*INS*), solute carrier family 2 (*SLC2A2*), and *HNF1A* (11). However, the expression of these genes was unchanged in the islets of β-cell-specific HNF4α knock-out (βHNF4α KO) mice (7, 8), indicating that such genes are not targets of HNF4α *in vivo*, at least in β-cells.

In the present study, we investigated the mRNA expression profile of βHNF4α KO mice and found that ankyrin repeat and sterile α motif domain containing 4b/harmonin-interacting, ankyrin repeat-containing protein (Anks4b/Harp) is a target of HNF4α in β-cells. We also demonstrated that Anks4b interacts with glucose-regulated protein 78 (GRP78), a major chaperone protein that protects cells from endoplasmic reticulum (ER) stress *in vitro* and *in vivo*. Gain- and loss-of-function studies of Anks4b revealed that it regulates sensitivity to thapsigargin (TG)-induced ER stress and apoptosis in MIN6 β-cell line. Our results suggest that HNF4α plays an important role in the regulation of ER stress and apoptosis in pancreatic β-cells.

EXPERIMENTAL PROCEDURES

Microarray Expression Profiling and HNF4α Motif Scan—Mice were maintained on a 12-h light/12-h dark cycle and allowed free access to food and water. All animal experiments were conducted according to the guidelines of the Institutional Animal Committee of Kumamoto University. Pancreatic islets were isolated from 45-week-old female βHNF4α KO mice (n = 5) and control flox/flox mice (n = 5) by collagenase digestion (12). Total RNA was prepared from the isolated islets with an RNeasy micro kit (Qiagen) according to the manufacturer's instructions, and its quality was confirmed by using an Agilent 2100 Bioanalyzer (Agilent Technologies, Palo Alto, CA). DNA microarray analysis was performed by the Kurabo GeneChip custom analysis service with GeneChip mouse genome 430 2.0 array (Affymetrix Inc., Santa Clara, CA). For identification of potential HNF4α binding sites, 5 kb of the promoter sequence upstream of the transcriptional start site was retrieved from the University of California Santa Cruz Genome Browser, and the sequence was analyzed by using the Transcription Element Search System (TESS) and the HNF4 Motif Finder generated by Sladek and colleagues (38).

Quantitative RT-PCR—Total RNA was extracted using an RNeasy micro kit (catalog number 74004, Qiagen, Valencia, CA) or Sepasol-RNA I super reagent (Nacalai Tesque, Kyoto, Japan). Then 1 μg of total RNA was used to synthesize first-strand cDNA with a PrimeScript RT reagent kit and gDNA Eraser (RR047A, TaKaRa Bio Inc., Shiga, Japan) according to the manufacturer's instructions. Quantitative real-time PCR was performed using SYBR *Premix Ex Taq* II (RR820A, TaKaRa) in an ABI 7300 thermal cycler (Applied Biosystems, Foster City, CA). The specific primers employed are shown in supplemental Table 1. Relative expression of each gene was normalized to that of TATA-binding protein.

Cell Lines and Culture—The MIN6 pancreatic β-cell line was cultured in Dulbecco's modified Eagle's medium (DMEM) containing 25 mM glucose, 15% fetal bovine serum, 0.1% penicillin/streptomycin, and 50 μM 2-mercaptoethanol at 37 °C under 5% CO_2, 95% air (13). HEK293, HeLa, and COS-7 cells were purchased from the American Type Culture Collection (ATCC) and were cultured in DMEM containing 2.5 mM glucose, 10% fetal bovine serum, and 0.02% penicillin/streptomycin.

Western Blotting—Cells were lysed in radioimmunoprecipitation assay buffer (50 mM Tris-HCl (pH 8.0), 150 mM NaCl, 0.1% SDS, 1% Nonidet P-40, 5 mM EDTA, 0.5% sodium deoxycholate, 20 μg/ml Na_3VO_4, 10 mM NaF, 1 mM PMSF, 2 mM DTT, and protease inhibitor mixture (1/100)) from Nacalai Tesque. Total protein was separated by SDS-polyacrylamide gel electrophoresis, transferred to a polyvinylidene fluoride (PVDF) membrane (Immobilon-P; Millipore, Bedford, MA), and probed with primary antibodies. After incubation with the secondary antibodies, the proteins were visualized using Chemi-Lumi One Super (Nacalai Tesque) and a LAS-1000 imaging system (Fuji Film, Tokyo, Japan). The primary antibodies used in this study were as follows: anti-HNF4α (1:1000) (H1415; Perseus Proteomics, Tokyo, Japan), anti-β-actin (1:2000) (A5441; Sigma-Aldrich), anti-harmonin (SAB250188; Sigma-Aldrich) (1:1000), anti-cleaved caspase-3 (Asp-175) (1:1000) (antibody 9661, Cell Signaling), and anti-GRP78 (1:1000) (sc-1051, Santa Cruz Biotechnology or antibody 4332, Cell Signaling).

Anti-Anks4b antiserum was generated by using a peptide that formed the central region of mouse Anks4b protein (amino acid residues 147–344). The nucleotide sequence of the peptide was amplified by PCR using a pair of primers (5′-CGGATC-CCCATGAAAGAGTGCGAACGGCTT-3′ and 5′-CGGATC-CCCTTACCATTCTACTTCTTCTTC-3′), and then it was subcloned into the pET28C+ vector. After expression in *Escherichia coli* BL21 (DE3), the His-tagged peptide was purified with His binding resin (Novagen) according to the manufacturer's instructions and dialyzed in a buffer containing 20 mM Tris-HCl (pH 8.0) and 500 mM NaCl. Subsequently, this peptide was used to inoculate rabbits for the production of anti-Anks4b antiserum.

Transient Transfection and Luciferase Reporter Assay—The mouse Anks4b promoter containing a putative HNF4α binding site was amplified by PCR using a pair of primers (5′-AGTGG-TCATTGCCATGGTTGGT-3′ and 5′-AGGTAGGAGTCTT-TGTCTAGGC-3′), and then it was subcloned into the pGL3 basic reporter (Promega). Transcription binding sites were altered by PCR-based mutagenesis to produce an HNF4α binding site mutant (GAACGGGGGCC) and an HNF1α binding site mutant (CTGACCGGCCAG). CD1b-HNF4α is a dominant negative mutant of HNF4α lacking the AF-2 activation domain (3). As described previously (14), the CD1b mutation was introduced by PCR into pcDNA3-HNF4α7 (kindly provided by Dr. Toshiya Tanaka, Tokyo University). The pcDNA3.1-wild-type (WT)-HNF1α and pcDNA3.1-P291fsinsC-HNF1α expression plasmids have been described previously (15). MIN6 cells or HEK293 cells (3×10^5 cells each) were seeded into 24-well plates at 18 h before transfection. Transient transfection was performed using Lipofectamine 2000 (Invitrogen) or X-treme GENE (Roche Applied Science) according to the manufacturer's instructions. At 24 h after transfection, luciferase activity was measured by using a Dual-Luciferase reporter assay system (Promega).

EMSA—A nuclear extract of MIN6 cells was prepared as described previously (16). Then 5 μg of the nuclear extract was incubated with ^{32}P-radiolabeled oligonucleotides containing the HNF4α or HNF1α binding sequence in a mixture containing 10 mM Tris-HCl (pH 7.5), 1% Ficoll, 70 mM KCl, 30 mg/ml BSA, 4.8% glycerol, and 100 μg/ml poly(dI-dC). Next, the DNA-protein complexes were resolved on 4% polyacrylamide gel in 0.5× Tris-borate-EDTA buffer at 120 V for 2 h, after which the dried gel was exposed to a phosphorimaging screen and analyzed with a BAS 2000 (Fuji Film). The oligonucleotide sequences were as follows: wild-type HNF4α binding site (5′-GGCCGGAGTGAACTTTGGCCTGGGGTGATA-3′); mutant HNF4α binding site (5′-GGCCGGAGTGAATGGGAGCCTGGGGTGATA-3′); wild-type HNF1α binding site (5′-CCCCGTCACTGATTAACCAGCCCTGTTGGA-3′); and mutant HNF1α binding site (5′-CCCCGTCACTGACCGGCCAGCCCTGTTGGA-3′). An anti-HNF1 antibody (H205, sc-8986) was used for the supershift assay.

Chromatin Immunoprecipitation—MIN6 cells were fixed in DMEM containing 1% formaldehyde for 10 min at room temperature, and then cross-linking was quenched by placing the cells in 200 mM glycine for 5 min at room temperature. The cells were incubated in Nonidet P-40 buffer (10 mM Tris-HCl (pH 8.0), 10 mM NaCl, 0.5% Nonidet P-40) for 5 min at room temperature and then lysed in SDS lysis buffer (50 mM Tris-HCl (pH 8.0), 1% SDS, 10 mM EDTA) followed by 5-fold dilution in ChIP dilution buffer (50 mM Tris-HCl (pH 8.0), 167 mM NaCl, 1.1% Triton X-100, and 0.11% sodium deoxycholate). Sonication was performed with a Sonifier 150 (Branson). Soluble sheared chromatin (20 μg) was incubated overnight at 4 °C with magnetic beads (Invitrogen Dynabeads protein G) bound to 2 μg of anti-HNF4α antibody (Santa Cruz Biotechnology sc-6556), anti-RNA polymerase II monoclonal antibody (Active Motif), or control IgG (Cell Signaling Technology antibody 2729) followed by sequential washing with low salt radioimmunoprecipitation assay buffer (50 mM Tris-HCl (pH 8.0), 150 mM NaCl, 1 mM EDTA, 0.1% SDS, 1% Triton X-100, and 0.1% sodium deoxycholate), high salt radioimmunoprecipitation assay buffer (50 mM Tris-HCl (pH 8.0), 500 mM NaCl, 1 mM EDTA, 0.1% SDS, 1% Triton X-100, and 0.1% sodium deoxycholate), wash buffer (50 mM Hepes-KOH (pH 7.5), 500 mM LiCl, 1 mM EDTA, 1% Nonidet P-40, and 0.7% sodium deoxycholate), and Tris-EDTA. Then immune complexes were eluted from the magnetic beads by incubation with ChIP direct elution buffer (50 mM Tris-HCl (pH 8.0), 10 mM EDTA, and 1% SDS) for 20 min at 65 °C. For reverse cross-linking, the eluate was incubated overnight at 65 °C, and then DNA fragments were purified by using a PCR purification kit (Qiagen). PCR was performed to identify Anks4b promoter fragments in the immunoprecipitated DNA using a pair of primers (5′-TTCACCACACTCATGACACACC-3′ and 5′-AGGTAGGAGTCTTTGTCTAGGC-3′).

GST Pulldown Assay—Mouse Anks4b cDNA was amplified by PCR using a pair of primers (5′-CGGATCCCCATGTCTACCCGCTATCACCAA-3′ and 5′-CGGATCCTTAGAGGCTGGTGTCAACCAACT-3′) and was subcloned into the pGEX4T2 vector (GE Healthcare). Anks4b deletion mutants (N-Anks4b (amino acid residues 1–126), M-Anks4b (amino acid residues 127–345), and C-Anks4b (amino acid residues 346–423)) were also generated by PCR and subcloned into the pGEX4T3 vector (GE Healthcare). GST-Anks4b proteins were expressed in *E. coli* BL21 (DE3) and purified with glutathione-Sepharose 4B beads (GE Healthcare). GST or GST fusion proteins (20 μg) immobilized on glutathione-Sepharose beads were incubated with 500 μg of mouse liver lysate. After binding overnight at 4 °C, the beads were washed with lysis buffer containing 10 mM Tris-HCl (pH 7.4), 150 mM NaCl, 1% Nonidet P-40, 1 mM EDTA, 10 mM NaF, 10 mM $Na_4P_2O_7$, 1 mM PMSF, and protease inhibitor mixture (Nacalai Tesque). Then the bound proteins were separated by SDS-PAGE.

Proteomic Identification of Anks4b-interacting Proteins—Silver-stained gels were subjected to in-gel digestion followed by extraction of peptides and proteomic analysis by LC-MS/MS. Gel digestion and peptide extraction were performed as reported previously (17). The peptide samples thus obtained were analyzed in an ESI-Q-TOF tandem mass spectrometer (6510; Agilent) with an HPLC chip-MS system, consisting of a nano pump (G2226; Agilent) with a four-channel microvacuum degasser (G1379B; Agilent), a microfluidic chip cube (G4240; Agilent), a capillary pump (G1376A; Agilent) with degasser (G1379B; Agilent), and an autosampler with thermostat (G1377A; Agilent). All modules were controlled by MassHunter software (version B.02.00; Agilent). A microfluidic reverse-phase-HPLC chip (Zorbax 300SB-C18; 5-μm particle size, 75-mm inner diameter, and 43 mm in length) was used for separation of peptides. The nano pump was employed to generate gradient nano flow at 600 nl/min, with the mobile phase being 0.1% formic acid in MS-grade water (solvent A) and 0.1% formic acid in acetonitrile (solvent B). The gradient was 5–75% solvent B over 9 min. A capillary pump was used to load samples with a mobile phase of 0.1% formic acid at 4 μl/min. The Agilent ESI-Q-TOF was operated in the positive ionization mode (ESI+), with an ionization voltage of 1,850 V and a fragmentor voltage of 175 V at 300 °C. Fragmentation of protonated molecular ions was conducted in the auto-MS/MS mode, starting with a collision energy voltage of 3 V that was increased by 3.7 V per 100 Da. The selected m/z ranges were 300–2,400 Da in the MS mode and 59–3,000 Da in the MS/MS mode. The data output consisted of one full mass spectrum (with three fragmentation patterns per spectrum) every 250 ms. The three highest peaks of each MS spectrum were selected for fragmentation. Mass lists were created in the form of Mascot generic files and were used as the input for Mascot MS/MS ion searches of the National Center for Biotechnology Information nonredundant (NCBI nr) database using the Matrix Science Web server Mascot version 2.2. Default search parameters were as follows: enzyme, trypsin; maximum missed cleavage, 1; variable modifications, carbamidomethyl (Cys); peptide tolerance, ± 1.2 Da; MS/MS tolerance, ± 0.6 Da; peptide charge, 2+ and 3+; instrument, ESI-Q-TOF. For positive identification, the result of $(-10 \times \log(p))$ could not exceed the significance threshold ($p < 0.05$).

Immunoprecipitation—Mouse Anks4b cDNA was amplified by PCR using a pair of primers (5′-CGGATCCCCATGTCTACCCGCTATCACCAA-3′ and 5′-CGGATCCTTAGAGGCTGGTGTCAACCAACT-3′) and was subcloned in-frame

into the pcDNA3-HA and pcDNA3-FLAG expression vectors. The GRP78 expression vector (pCMV-BiP-Myc-KDEL-wt) was a gift from Dr. Ron Prywes (Addgene plasmid 27164). After transfection into COS-7 cells, the cells were lysed in immunoprecipitation buffer (20 mM Tris-HCl (pH 7.4), 175 mM NaCl, 2.5 mM $MgCl_2$, 0.05% Nonidet P-40, 1 mM PMSF, and protease inhibitor mixture (Nacalai Tesque)) and incubated on ice for 30 min. Then 700 μg of cell lysate and FLAG tag antibody beads (Wako) were mixed and stirred at 4 °C for 18 h. After washing with immunoprecipitation buffer, proteins were eluted by using DYKDDDDK peptide (Wako). A sample of the eluate and 2% of the cell lysate (from before processing) were subjected to Western blotting analysis.

Immunocytochemistry—Both the pcDNA3-HA-Anks4b and the pCMV-BiP-Myc-KDEL-wt vectors were transfected into HeLa, COS-7, and MIN6 cells with X-treme GENE (Roche Diagnostics) for 24 h. Then the cells were fixed in 10% neutralized formalin and permeabilized with 0.1% Triton X-100, 3% BSA/PBS. Monoclonal rat anti-HA antibody (1:400) (clone 3F10, Roche Applied Science) and mouse anti-c-Myc antibody (1:400) (Wako) were used as the primary antibodies, whereas Alexa Fluor 568 goat anti-rat IgG (Invitrogen) and Alexa Fluor 488 goat anti-mouse IgG (Invitrogen) were used as the secondary antibodies. Immunofluorescence was detected under a laser scanning confocal microscope (FV-1000, Olympus, Tokyo, Japan).

Retrovirus Infection—Mouse Anks4b and human HNF4α7 cDNAs were subcloned into the pMXs-puro retrovirus vector for overexpression (18). Specific shRNA sequences for mouse HNF4α (5′-CCAAGAGCTGCAGATTGAT-3′) and Anks4b (5′-GAAGAAGACTCATTTCCAA-3′) were designed using the Clontech RNAi target sequence selector. Oligonucleotides encoding shRNA were synthesized and cloned into the pSIREN-RetroQ retroviral shRNA expression vector (Clontech). Then the pMXs-Anks4b, pMXs-HNF4α7, and empty pMXs vectors were transfected into Plat-E cells using FuGENE6 (Roche Applied Science, Mannheim, Germany). For knockdown experiments, transfection was done with pSIREN-RetroQ-Anks4b, pSIREN-RetroQ-HNF4α, and the negative control pSIREN-RetroQ vector. MIN6 cells were infected with the retroviruses and selected by incubation with puromycin (5 μg/ml) (12).

Flow Cytometric Analysis—An annexin V-FITC apoptosis detection kit (BioVision Research Products, Mountain View, CA) was used for the apoptosis assay according to the manufacturer's instructions. MIN6 cells were cultured in DMEM for 30 h with or without 1 μM thapsigargin (Nacalai Tesque). After incubation in trypsin/EDTA for 10 min at 37 °C, cells were centrifuged at 6,000 rpm for 10 min. The pellet was resuspended in 1×resuspension buffer, and the cells were stained with annexin V-FITC antibody. After incubation for 5 min at room temperature in the dark, stained cells were analyzed using a FACSCalibur (BD Biosciences) and FlowJo software (Tomy Digital Biology, Tokyo, Japan).

Statistical Analysis—Statistical analyses were performed using Statview J-5.0 software (SAS Institute, Cary, NC). The significance of differences was assessed with the unpaired *t* test, and $p < 0.05$ was considered to indicate statistical significance.

RESULTS

Anks4b Is a Novel Target of HNF4α—To identify target genes of HNF4α in pancreatic β-cells, DNA microarray analysis was performed using islets from βHNF4α KO mice and control mice. Body weight and blood glucose levels were similar for these two strains of mice (body weight was 32.7 ± 1.7 g ($n = 5$) *versus* 34.1 ± 1.9 g ($n = 5$) and random blood glucose was 128 ± 27 mg/dl ($n = 5$) *versus* 114 ± 24 mg/dl ($n = 5$) for βHNF4α KO *versus* control mice). Microarray analysis identified 56 up-regulated genes (signal log ratio ≥2) and 100 down-regulated genes (signal log ratio ≤−1.5) in βHNF4α KO islets (supplemental Table 2). Expression of the majority of the genes known to be involved in glucose metabolism was unchanged. To validate these results, expression of mRNA for genes randomly chosen from both the down-regulated and the up-regulated groups was assessed by quantitative real-time PCR in an independent group of 12-week-old male mice. As a result, differential expression of most genes was confirmed (Fig. 1*A* and supplemental Fig. 1). Gupta *et al.* (19) reported that ST5, a regulator of ERK activation, is a direct target of HNF4α in β-cells. Expression of ST5 mRNA was reduced by 24.6% in βHNF4α KO islets (supplemental Fig. 2).

Next, we performed a computational scan of the HNF4α binding motif in the down-regulated genes. This identified 22 high affinity HNF4α binding sequences in the mouse promoter. In 3 out of 22 genes, the HNF4 motif was also conserved in the corresponding human genome. These three genes encoded *Anks4b*, guanylate cyclase 2c (*Gucy2c*), and peroxisome proliferator-activated receptor γ coactivator-1α (*Ppargc1a*). Quantitative real-time PCR analysis confirmed a significant decrease of Anks4b expression in the islets of 12-week-old βHNF4α KO mice (17.3% of the control level, $p < 0.01$) (Fig. 1*B*). In contrast, the reduction of Gucy2c mRNA expression was marginal (21.7% of the control level, $p = 0.06$), and *Ppargc1a* mRNA levels were unchanged. The difference of sex and age of mice or different detection systems might have contributed to the different results. To elucidate the direct effect of HNF4α on the expression of these three genes, we established MIN6 β-cells that stably expressed HNF4α-specific shRNA (HNF4α KD-MIN6) by retroviral infection. Suppression of endogenous HNF4α was confirmed at both the mRNA and the protein levels (Fig. 1*C*). Decreased expression of *Anks4b*, *Gucy2c*, and *Ppargc1a* was found in HNF4α KD-MIN6 cells (Fig. 1*D*). Because *Anks4b* gene expression was most markedly decreased in both βHNF4α KO islets and HNF4α KD-MIN6 cells (35.2% of the control level, $p < 0.001$), we focused on Anks4b for further investigation.

Screening of the promoter region of the mouse Anks4b gene by using a genomic databank revealed an HNF4α binding site (nucleotides −108 to −120 relative to the translation start codon when A is designated as +1). We cloned a 190-bp promoter region upstream of a luciferase reporter gene and co-expressed it with the HNF4α expression vector in HEK293 cells. Induction of HNF4α7 (an isoform expressed in pancreatic β-cells (4)) increased Anks4b promoter activity in a concentration-dependent manner (Fig. 2*A*), whereas overexpression of the HNF4α mutant lacking AF-2 had no effect (Fig. 2*B*). When

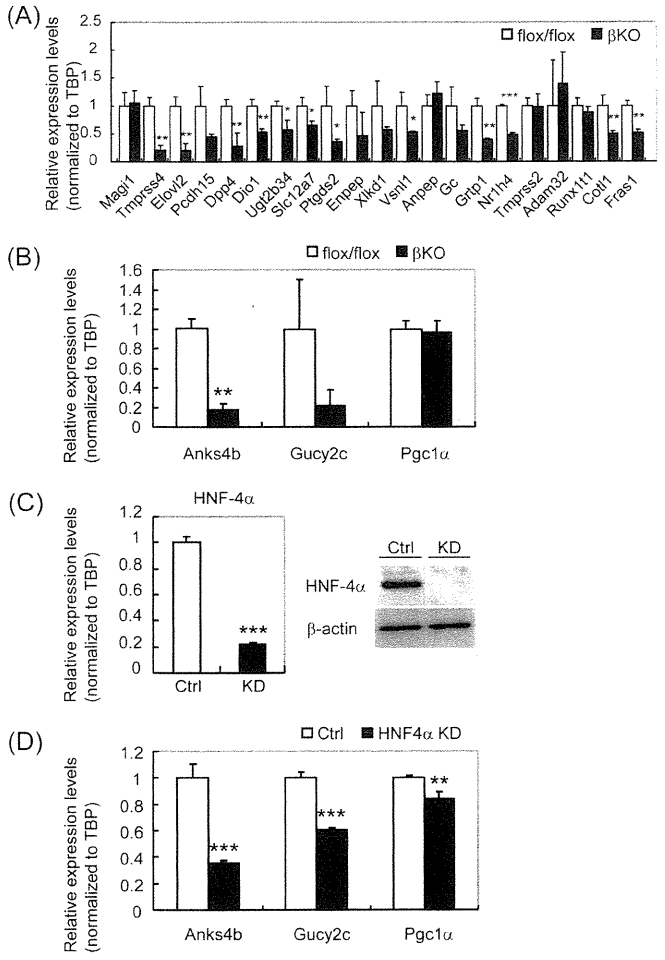

FIGURE 1. **Gene expression in the islets of βHNF4α KO mice and HNF4α knockdown MIN6 cells.** *A*, quantitative RT-PCR analysis of genes randomly chosen from those in supplemental Table 1 using flox/flox control (*white bar*) and βHNF4α KO islets (*black bar*, male, 12 week, $n = 4$). Expression of each gene was normalized for that of TATA-binding protein (*TBP*). *B*, expression of *Anks4b*, *Gucy2c*, and *Ppargc1a* in βHNF4α KO islets. Decreased expression of Anks4b was confirmed by quantitative RT-PCR. *C*, HNF4α mRNA (*left*) and HNF4α protein (*right*) in control (*Ctrl*, *white bar*) and HNF4α knockdown MIN6 cells (*KD*, *black bar*) were evaluated by quantitative PCR ($n = 4$) and Western blotting, respectively. β-Actin was used as the loading control. *D*, expression of *Anks4b*, *Gucy2c*, and *Ppargc1a* was significantly decreased in HNF4α KD-MIN6 cells. The mean ± S.D. for each group is shown (*, $p < 0.05$, **, $p < 0.01$, ***, $p < 0.001$).

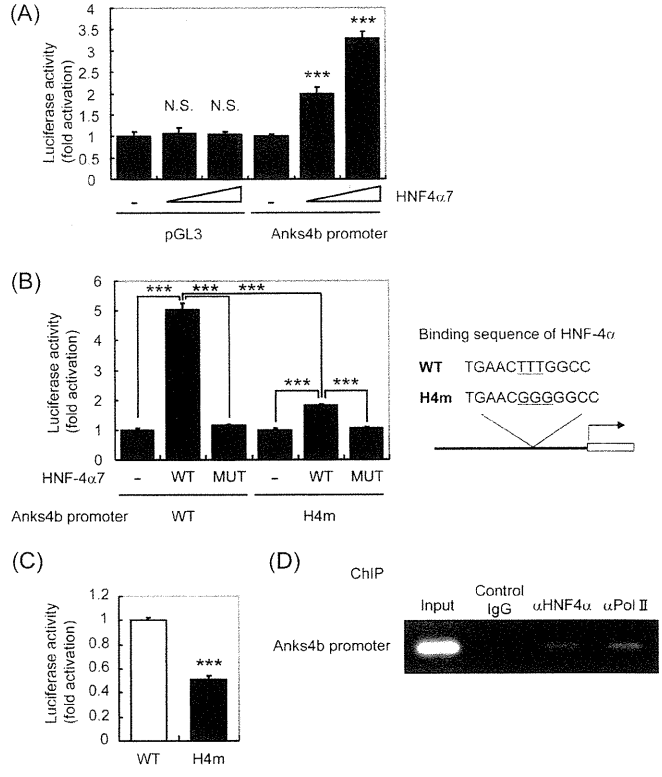

FIGURE 2. **Transcriptional regulation of Anks4b by HNF4α.** *A*, HEK293 cells were cotransfected with the pcDNA3-HNF4α7 expression vector (0–75 ng), as well as 50 ng of pGL3 basic or pGL3-Anks4b reporter and 25 ng of pRL-TK. *B*, HEK293 cells were cotransfected with 50 ng of pcDNA3-wild-type-HNF4α7 (WT) or pcDNA3-mutant (MUT) HNF4α7, as well as 50 ng of pGL3-Anks4b reporter (WT and MUT) and 25 ng of pRL-TK. *C*, MIN6 cells were transfected with pGL3-Anks4b reporter (WT and MUT) and 25 ng of pRL-TK. The mean ± S.D. for each group ($n = 3$) is shown (***, $p < 0.001$). *N.S.*, not significant. *D*, chromatin immunoprecipitation assay with MIN6 cells. Interaction of HNF4α with the promoter of Anks4b was observed. *αPol II*, RNA polymerase II antibody.

the putative HNF4α binding site in the Anks4b promoter was subjected to mutation (H4m), transcriptional activation by HNF4α7 was significantly reduced by 64.0% ($p < 0.001$) (Fig. 2*B*). Disruption of the HNF4α binding site was also associated with a 48.5% reduction of promoter activity in MIN6 cells ($p < 0.001$) (Fig. 2*C*). To assess the binding of HNF4α to the Anks4b promoter, a chromatin immunoprecipitation (ChIP) assay was performed using MIN6 cells. This assay revealed binding of HNF4α to the Anks4b promoter of MIN6 cells (Fig. 2*D*). Specific binding of HNF4α to the putative binding site was also demonstrated by the electrophoretic mobility shift assay (EMSA) (supplemental Fig. 3). Thus, both *in vivo* and *in vitro* data indicated that Anks4b is a direct target of HNF4α in β-cells.

HNF4α and HNF1α Synergistically Activate Transcription of Anks4b—HNF1α is a homeodomain-containing transcription factor that is also expressed in the liver, kidney, intestine, and pancreas (20). Mutation of the *HNF1A* gene causes another type of MODY known as MODY3 (21). In addition to the binding site for HNF4α, we also found an HNF1α binding consensus sequence in the Anks4b promoter (Fig. 3*A*). Therefore, we examined the role of HNF1α in Anks4b gene transcription. First, binding of HNF1α to the Anks4b gene was examined by EMSA with MIN6 nuclear extracts and a probe corresponding to the HNF1α binding site (Fig. 3*B*). The probe shifted after the addition of nuclear extracts (*lane 2*), and its binding was blocked by the addition of a 30-fold excess of unlabeled oligonucleotide (*lane 3*). Specificity of HNF1α binding was assessed by supershifting the DNA-HNF1α complex using HNF1α antibody (*lane 5*), indicating that HNF1α also binds directly to the Anks4b promoter. To examine the influence of HNF1α on Anks4b gene expression, we next performed a reporter gene assay. WT-HNF1α caused a dose-dependent increase of Anks4b promoter activity (Fig. 3*C*). Interestingly, Anks4b mRNA expression was decreased in HNF1α KO islets according to the results of DNA microarray analysis (22). Taken together, these results suggested that Anks4b is a target of

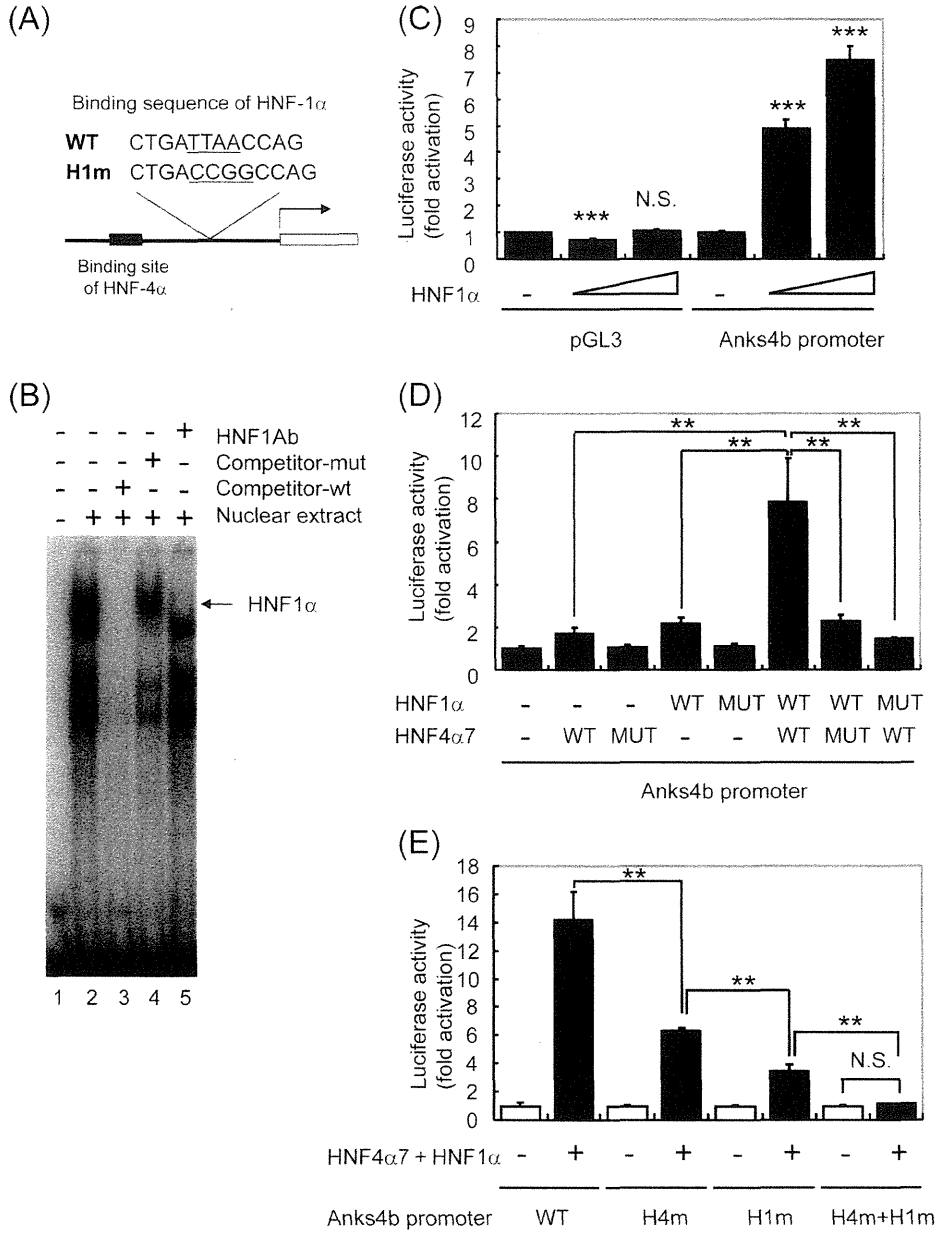

FIGURE 3. **Synergistic activation of Anks4b transcription by HNF4α and HNF1α.** *A*, DNA sequences of the promoter region of the mouse and human Anks4b genes. The putative HNF4α and HNF1α binding sites are shown. *B*, EMSA analysis of the HNF1α binding site in the Anks4b gene. DNA binding was tested using nuclear extracts from MIN6 cells. *C*, HEK293 cells were cotransfected with the pcDNA3.1-HNF1α expression vector (0–75 ng), as well as 50 ng of pGL3 basic or pGL3-Anks4b reporter and 25 ng of pRL-TK. *D*, HEK293 cells were cotransfected with 10 ng of pcDNA3.1-HNF1α (WT or MUT) and 10 ng of pcDNA3-HNF4α7 (WT or MUT), as well as 50 ng of pGL3-Anks4b reporter and 5 ng of pRL-TK. *E*, HEK293 cells were cotransfected with pcDNA3.1-HNF1α and pcDNA3-HNF4α7 as well as 50 ng of pGL3-Anks4b reporter (WT or MUT). *H4m*, mutation of the HNF4α binding site; *H1m*, mutation of the HNF1α binding site. *H4m+H1m*, mutation of both binding sites. The mean ± S.D. for each group ($n = 3$) is shown (**, $p < 0.01$, ***, $p < 0.001$). *N.S.*, not significant.

HNF1α as well as HNF4α. Because it has been reported that HNF4α and HNF1α cooperatively activate target genes that have binding sites for both HNFs in the promoter region (23, 24), we examined the influence on Anks4b gene expression of interaction between HNF4α and HNF1α. When an Anks4b reporter construct was cotransfected into HEK293 cells with 10 ng of HNF1α or HNF4α expression plasmid, the reporter gene was activated by 2.2- and 1.7-fold, respectively (Fig. 3*D*). In contrast, there was a dramatic increase of promoter activity (7.9-fold) when both constructs were cotransfected simultaneously (Fig. 3*D*). Mutation of either HNF1α or HNF4α markedly suppressed this response (Fig. 3*D*). Synergistic activation of Anks4b promoter activity was significantly suppressed by disruption of either the HNF4α binding site (H4m) or the HNF1α binding site (H1m), and activation was completely abolished by both H4m and H1m (Fig. 3*E*). Taken together, these results indicate that Anks4b promoter activity is synergistically regulated by both HNF4α and HNF1α.

Anks4b Interacts with GRP78 Both in Vitro and in Vivo—Anks4b is a scaffold protein with three ankyrin repeats and a sterile α motif domain that was identified as harmonin-interacting protein (25), although its function is completely

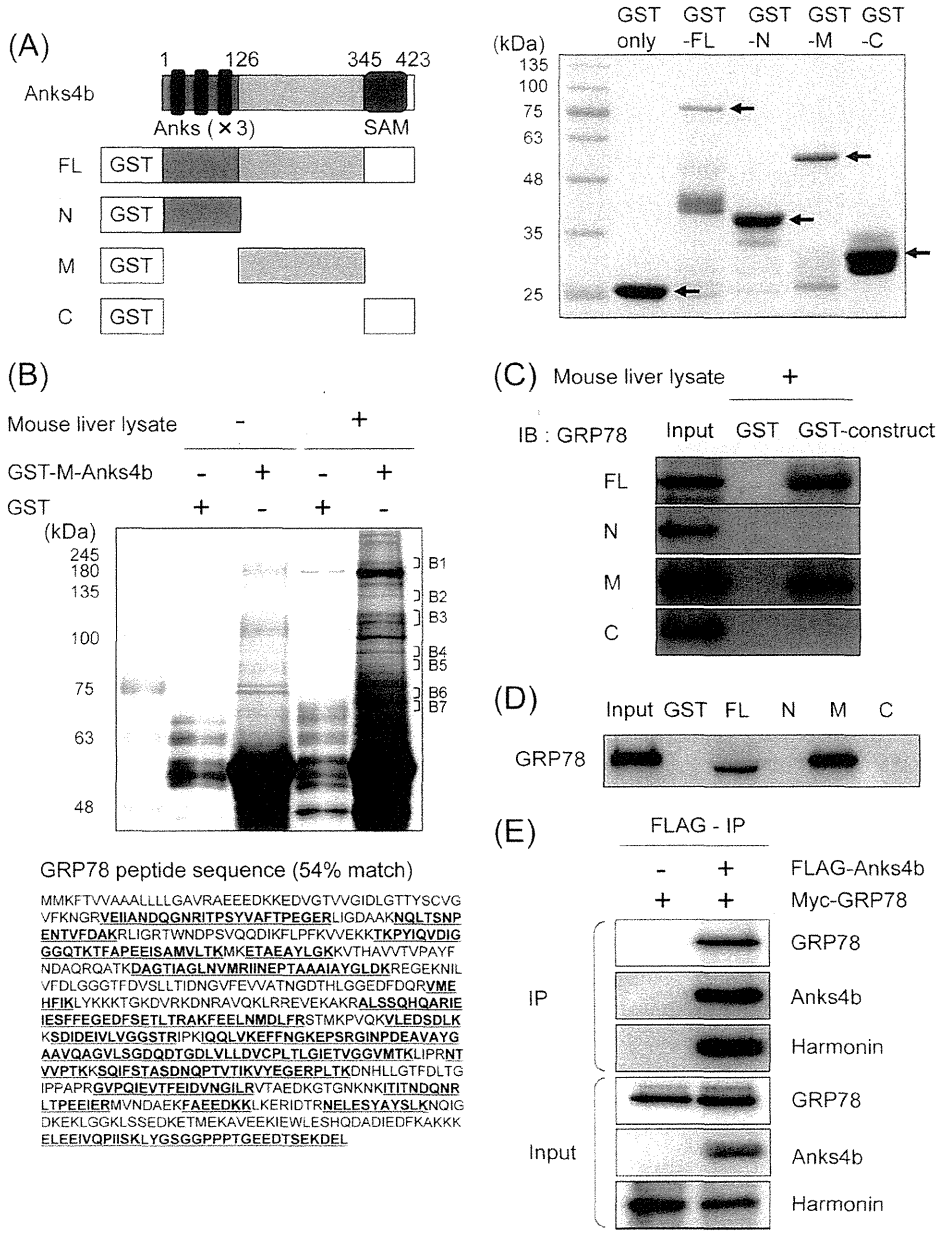

FIGURE 4. **Interaction of Anks4b and GRP78 *in vitro* and *in vivo*.** *A*, schematic representation of full-length Anks4b (*FL*) and deletion mutants of Anks4b (N-Anks4b (*N*), M-Anks4b (*M*), and C-Anks4b (*C*)) and expression of GST-Anks4b fusion proteins (Coomassie Brilliant Blue staining). *SAM*, sterile α motif. *B*, purification of proteins interacting with Anks4b. The GST pulldown assay using M-Anks4b was performed with mouse liver lysates. Eluted proteins were resolved by SDS-PAGE and then silver-stained. Seven regions (*B1–B7*) were excised for mass spectrometry. GRP78 residues were detected by mass spectrometry (*bold* and *underlined letters*). *C* and *D*, interaction of Anks4b and GRP78 *in vitro*. After the pulldown assay using mouse liver lysates (*C*) or MIN6 lysates (*D*), binding of GRP78 with FL- and M-Anks4b was detected by Western blotting (*IB*). *E*, interaction of Anks4b and GRP78 *in vivo*. COS-7 cells were transfected with the pCMV-Bip/GRP78-Myc-KDEL-wt or pCMV-Bip/GRP78-Myc-KDEL-wt and pcDNA3-FLAG-Anks4b expression vectors. Immunoprecipitation (*IP*) was performed with FLAG resin and 700 μg of COS-7 cell lysate.

unknown. To elucidate the role of Anks4b in β-cells, we searched for molecules that interacted with full-length Anks4b (FL) and with its deletion mutants (N-, M-, and C-Anks4b) (Fig. 4*A*) by performing a GST pulldown assay of mouse liver lysates (Fig. 4*B* and supplemental Fig. 4). We found a protein of ~75 kDa that specifically precipitated with GST-M-Anks4b (B6), and it was identified as GRP78/binding immunoglobulin protein (BiP) by mass spectrometry (Fig. 4*B*). GRP78 is an ER-localized chaperone protein that is induced by the unfolded protein response in response to ER stress (26, 27). Binding of GRP78 to GST-FL-Anks4b and GST-M-Anks4b, but not to GST, GST-N-Anks4b, or C-Anks4b, was confirmed by Western blotting using a specific antibody for GRP78 (Fig. 4*C*), suggesting that GRP78 bound to the middle region of Anks4b. GST pulldown experiments using MIN6 cell lysates also demonstrated binding of GRP78 to Anks4b (Fig. 4*D*).

Subsequently, we evaluated the interaction between Anks4b and GRP78 in cultured cells. COS-7 cells were transfected with the Myc-GRP78 expression plasmid alone or with Myc-GRP78 plus FLAG-tagged wild-type Anks4b expression plasmids, and

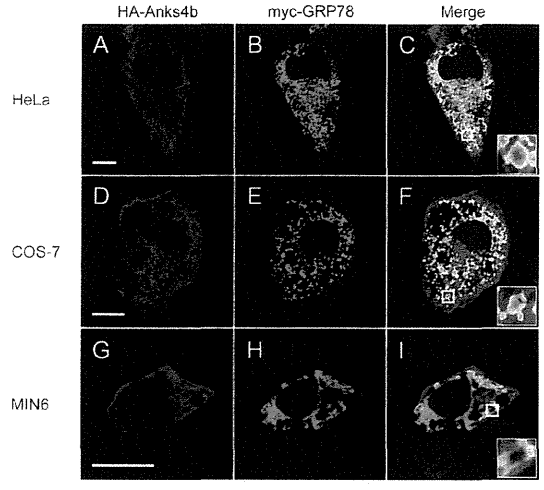

FIGURE 5. **Intracellular localization of Anks4b adjacent to the ER membrane.** *A–I*, HeLa (*A–C*), COS-7 (*D–F*), and MIN6 (*G–I*) cells were cotransfected with the pcDNA3-HA-Anks4b and pCMV-Bip/GRP78-Myc-KDEL-wt expression vectors. Cells were double-stained with anti-HA antibody (Alexa Fluor 563, *red*) and anti-Myc antibody (Alexa Fluor 488, *green*). DAPI (*blue*) was used for nuclear staining. *Insets* represent higher magnifications of the *boxed regions* in *C* (×18), *F* (×13), and *I* (×8). *Scale bar* = 10 μm.

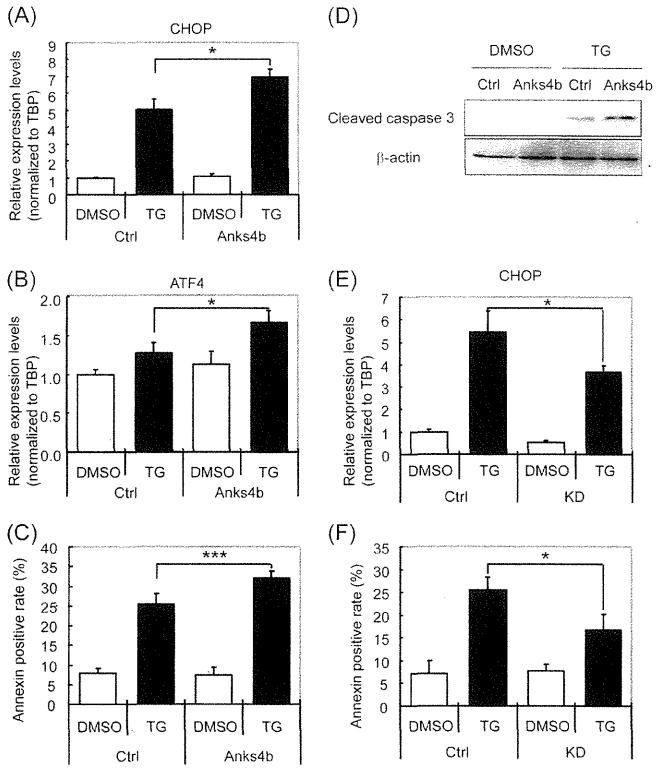

FIGURE 6. **Regulation of ER stress-mediated apoptosis by Anks4b.** *A* and *B*, MIN6 cells overexpressing Anks4b were cultured in the absence or presence of 1 μM thapsigargin for 20 h, and then quantitative RT-PCR was performed. *TBP*, TATA-binding protein. *DMSO*, dimethyl sulfoxide; *Ctrl*, control. *C*, MIN6 cells overexpressing Anks4b were cultured in the absence or presence of 1 μM thapsigargin for 30 h, and the percentage of annexin V-positive cells was analyzed by flow cytometry. *D*, Western blotting of cleaved caspase-3 after treatment with 1 μM thapsigargin for 20 h. *E*, Anks4b knockdown MIN6 cells were cultured for 20 h with 1 μM thapsigargin, and then quantitative RT-PCR was performed. *F*, annexin V-positive cells were analyzed after treatment of Anks4b knockdown MIN6 cells with 1 μM thapsigargin for 30 h. The mean ± S.D. for each group ($n = 4$) is shown (*, $p < 0.05$, **, $p < 0.01$, ***, $p < 0.001$).

cell lysates were immunoprecipitated with FLAG resin. As shown in Fig. 4*E*, FLAG-Anks4b was able to coimmunoprecipitate GRP78 as well as harmonin, a protein that was previously found to interact with Anks4b (25). These results indicated that Anks4b binds to GRP78 in cells.

Anks4b Colocalizes with GRP78 in the Endoplasmic Reticulum—We next investigated the intracellular localization of Anks4b. HA-tagged Anks4b and Myc-tagged GRP78 constructs were cotransfected into HeLa cells, and an immunofluorescence study was performed. HA staining (Anks4b, *red*) revealed a reticular pattern in the cytoplasm, but no signals were detected in the nucleus (Fig. 5*A*). Double staining for Anks4b and GRP78 (Myc, *green*) as a marker for the ER revealed that both signals were frequently colocalized (Fig. 5, *B* and *C*). In contrast, Anks4b staining did not overlap with MitoTracker, a specific marker for the mitochondria (supplemental Fig. 5). A similar staining pattern was also detected in COS-7 cells and MIN6 cells (Fig. 5, *D–I*). These findings were further evidence that Anks4b interacts with GRP78. Notably, Anks4b staining was detected at the periphery of the ER lumen (Fig. 5, *C*, *F*, and *I*, *inset*), suggesting that it was localized adjacent to the ER membrane.

Anks4b Regulates Apoptosis in Response to ER Stress—GRP78 is a major chaperone protein that protects cells from ER stress, and overexpression of GRP78 reduces ER stress-mediated apoptosis by attenuating the expression of C/EBP homologous protein (CHOP) (28, 29). Accordingly, detection of an interaction between Anks4b and GRP78 prompted us to investigate the role of Anks4b in both ER stress and apoptosis. TG causes ER stress by preventing calcium uptake from the cytoplasm into the ER (30), and treatment of MIN6 cells with 1 μM TG for 20 h increased the expression of the ER stress-related genes (ATF4, spliced XBP1, and CHOP) (data not shown). First, we examined the effect of Anks4b overexpression on MIN6 cells (supplemental Fig. 6). Anks4b overexpression did not affect CHOP gene expression in the absence of TG, but TG-induced CHOP expression was significantly increased (1.4-fold, $p < 0.05$) (Fig. 6*A*). TG-induced ATF4 expression was also significantly augmented in Anks4b-overexpressing MIN6 cells (1.3-fold, $p < 0.05$) (Fig. 6*B*). Furthermore, the number of annexin V-positive apoptotic cells was increased by overexpression of Anks4b (1.3-fold, $p < 0.001$) (Fig. 6*C*). Augmentation of apoptosis was also observed in MIN6 cells overexpressing HNF4α7 (supplemental Fig. 7). Activation of caspase-3 mediates the induction of apoptosis downstream of CHOP (31), and activated (cleaved) caspase-3 protein expression was increased when Anks4b-overexpessing MIN6 cells were treated with TG (Fig. 6*D*).

Next, we examined the effect of knockdown of Anks4b in MIN6 cells (supplemental Fig. 8). Suppression of endogenous Anks4b mRNA by shRNA in MIN6 (reduced to 40.5% of the control level) did not affect CHOP gene expression in the absence of TG, but TG-induced CHOP expression was significantly reduced by 32.1% ($p < 0.05$) (Fig. 6*E*). In addition, flow cytometric analysis using annexin V revealed that TG-induced apoptosis was also decreased by suppression of Anks4b (Fig. 6*F*). Collectively, these findings indicate that Anks4b promotes the induction of ER stress and apoptosis by TG in MIN6 cells.